صنایع زیست‌فرایندی در دهه‌های گذشته کارآیی فناورانهٔ خود را به‌خوبی نشان داده‌اند. گلویی عملکردی اینگونه فرایندها در نحوهٔ کنترل موثر و ابزاردقیق آنها نهفته است. علت نیز عملکرد پیچیده، طبیعی و شدیداً غیرخطی موجودات زنده است. هدف از این پروژه، تمرین طراحی کنترلر و سنسور نرم‌افزاری با استفاده از یک بیوراکتور نمونه است.

برای کمّی‌کردن مسئله، از فصل بیست و سوم کتاب سیبورگ و همکاران (نگارش چهارم)[1] کمک گرفته و مثال ۲۳.۱ (یعنی راکتور حجم ثابت) را مبنا قرار می‌دهیم. مطلوبی‌های پروژه به‌شرح زیر هستند؛

۱۰ **(الف)** مطابق الگوی عمل‌شده در کارگاه نرم‌افزار[2] (فایل MatlabTutorialPart5.pdf) فایلهای فانکشن و اسکریپت برای خطی‌سازی سیستم مثال ۲۳.۱ را تهیه و گزارش کنید. <mark>تهیهٔ فانکشنها و اسکریپتهای Live در زمره نمرات تشویقی بشمار می‌روند.</mark>

۱۰ **(ب)** نمودار بهرهٔ یکنواخت را رسم کرده و نشان دهید در نقاط کاری مختلف، بهرهٔ فرایند تغییر علامت می‌دهد. برای رسم نمودار، خروجی قابل اندازه‌گیری را حالت غلظت زیست توده (X) و ورودی (کنترل‌کننده) را همان نرخ رقیق‌سازی (D) در نظر بگیرید.

۱۰ **(ج)** بخش اول مثال (بخش **a**) را بازتکرار کرده و نتیجه را گزارش کنید.

۱۰ **(د)** پاسخ مدارباز تمامی حالات به تغییر ۱۰٪± در نرخ رقیق‌سازی را یکبار در نقطهٔ کاری $D = 0.202\ hr^{-1}$ (نرخ ترقیق بالا) و یکبار در نقطهٔ کاری $D = 0.0389\ hr^{-1}$ (نرخ ترقیق پایین) رسم کنید. دقت شود، مقادیر تعادلی حالات را می‌توانید (بطور دلبخواه) از توابع trim متلب[3] یا حل غیرخطی سه معادله–سه مجهول به‌دست آورید. <mark>تغییرات بیشتر از ۱۰٪± به‌صورت تشویقی محسوب می‌شوند.</mark>

۱۰ **(ه)** با استفاده از مرکز تنظیم کنترلر سیمیولینک، یک کنترلر تناسبی–انتگرالی برای جفت (X,D) در نقطهٔ کاری «نرخ ترقیق پایین» طراحی کنید. پاسخ مداربسته را برای دفع اغتشاش ۱۰٪± درصدی در غلظت جریان شربت قند بالادستی (S_f) به‌دست آورید.

۱۰ **(و)** برای امتحان تاب‌آوری (مقاومت) کنترلر طراحی‌شده در قسمت قبل، تغییر در مقدار مقرر را طوری تعیین و امتحان کنید که سیستم وارد نقاط کاری‌ای شود که بهرهٔ آن تغییر علامت دهد.

۲۰ **(ز)** یک کنترلر پیشخور (فیدفوروارد) که از اطلاعات سنجش غلظت گلوکز خوراک (S_f) در ترکیب با کنترلر پسخور قسمت **(ه)** استفاده می‌کند، طراحی کنید. برای مقایسه و مشاهدهِ بهبود عملکرد، پاسخ تغییرات حالتِ مداربستهٔ کنترلر دو درجهٔ آزادی (پیشخور–پسخور) را در کنار نتایج کنترلر فقط پسخورِ قسمت **(ه)** گزارش کنید. تعداد و فرمت نمودارها به‌شرح متعاقب است؛ تعداد هشت نمودار سری زمانی (مقدار سیگنال برحسب زمان) که چهارتای آن مربوط به رفتار سه حالت و یک رفتار نرخ رقیق‌سازی در دفع اغتشاش افزایشی (۱۰٪+) و چهارتای دیگر برای دفع اغتشاش کاهشی (۱۰٪-) باشد. بدیهیست، هرکدام از این هشت نمودار باید بصورت جفت سیگنالی، یعنی یک سیگنال با خط توپر متعلق به حلقهٔ ترکیبی (پیشخور–پسخور) و دیگری بصورت خطچین متعلق به حلقهٔ پسخور باشد.

۲۰ **ح)** برای دو حالت زمان نمونه‌برداری نیم‌ساعته و یک‌ونیم ساعته دو کنترلر فیدبک دائلین با شرط کمترین زمان نشست ممکن برای جفت (X,D) در نقطهٔ کاری «نرخ ترقیق پایین» طراحی کرده و نتایج عملکرد حذف اغتشاش آنها را گزارش کنید. <mark>طراحی کنترلر گسسته قطب‌گماری به‌صورت تشویقی محسوب می‌شوند.</mark>

قانون مورفی: در شرائط کنترلی بسیار دقیق دما، فشار، غلظت و سایر متغیرهای عملیاتی، موجودات زنده هر کاری که خودشان بخواهند انجام می‌دهند.

---

[1] Appendix I

[2] Appendix III

[3] Appendix IV

Chapter 23

Biosystems Control Design

CHAPTER CONTENTS

Previous chapters have introduced the concepts of process dynamics and strategies for process control, emphasizing traditional applications from the petrochemical industries, such as chemical reactors and distillation columns. In this chapter, we introduce the application fields of bioprocessing and biomedical devices, and elucidate the characteristics that these processes share with traditional chemical processes. Differences will also be highlighted, including the nature of uncertainty in biological processes, as well as the safety considerations in medical closed-loop systems. Control system design for three bioprocessing operations is described: crystallization, fermentation, and granulation. Finally, a number of problems in controlled drug delivery are reviewed, and control strategies are demonstrated in the areas of diabetes and blood pressure regulation. Biological applications are expanded in Chapter 24, with a discussion of control systems opportunities, including applications to systems biology.

23.1 PROCESS MODELING AND CONTROL IN PHARMACEUTICAL OPERATIONS

A typical flowsheet in the pharmaceutical industry contains many of the same categories of operations as occur in a traditional petrochemical processing plant: reactors to generate products from raw materials, purification steps to extract desired products from the by-products and unreacted feed materials, and downstream processing associated with the final formulation of the product. Pharmaceutical processes are unique in several respects: (1) the main reactions involve biological materials, such as cells and tissues from more complex organisms, and (2) most of the products are formulated in solid form, which requires a unique set of bulk solids processing steps to purify and formulate the desired end product (e.g., a medicinal tablet). Consequently, the upstream processing involves sterilization and fermentation, and the manipulated inputs for the reactor often include *inducers* to activate the expression of particular genes in microbes in the reactor (gene expression is covered in more detail in Chapter 24). The downstream section of the flowsheet includes crystallization or chromatographic purification, to extract a high-purity product with desirable properties (e.g., chirality). Subsequent steps may involve solids handling and processing to produce final particulates with desirable properties, including dissolution attributes and tableting capability. These processes include mixing, classification, milling, grinding, crushing, granulation (agglomeration), tableting, coating, molding, and extrusion. Each of these

operations has its own challenges and unique dynamic characteristics.

In the following sections, we consider three of the main processing steps in the pharmaceutical flowsheet: fermentation, crystallization, and granulation. Several of these processes appear in other industries as well (e.g., food, mining, semiconductor, and specialty chemical), so the process control methods described find broad application in industry. It is important to note that the industry has a new emphasis on process systems engineering methods, driven by changes in FDA regulations (see PAT discussion in Chapter 22). The pharmaceutical industry is placing increasing emphasis on integrated manufacturing, linking the control of synthesis, purification, and final (drug) product formulation (Mascia et al., 2013). Furthermore, the push for sustainable manufacturing has identified unique challenges and opportunities for this sector (Sheldon, 2007).

23.1.1 Bioreactors

Fermentation reactors are widely used in the pharmaceutical industries to make an array of important compounds, including penicillin, insulin, and human growth hormone. In recent years, genetic engineering has further expanded the portfolio of useful products that can be synthesized using fermentation methods (Buckland,

1984; Lim, 1991; Schügerl, 2001). Despite the importance of this unit operation, the state of pharmaceutical fermentation operations is often characterized as more art than science, as with the winemaking industry (Fleet, 1993; Alford, 2006). In beermaking, there are similar traditions of "art", although modern facilities employ a sophisticated array of unit operations (e.g., cooking, washing, lautering, brewing, fermentation) with the corresponding control challenges. Since 1990, there has been a focused effort to develop more sophisticated control architectures for fermentation operation, driven by the availability of new technologies for monitoring the quality of the contents of the fermentor (see, e.g., Van Impe et al., 1998; Boudreau and McMillan, 2007). Key measurements and their associated controlled variables include dissolved oxygen (status of aerobic metabolic process), pH (optimal growth conditions), temperature (metabolic heat generation), and offgas concentration (indicator of culture activity). A schematic of a fermentation process is given in Figure 23.1.

In a general sense, fermentation involves the generation of cell mass (product) from a substrate according to a simple reaction:
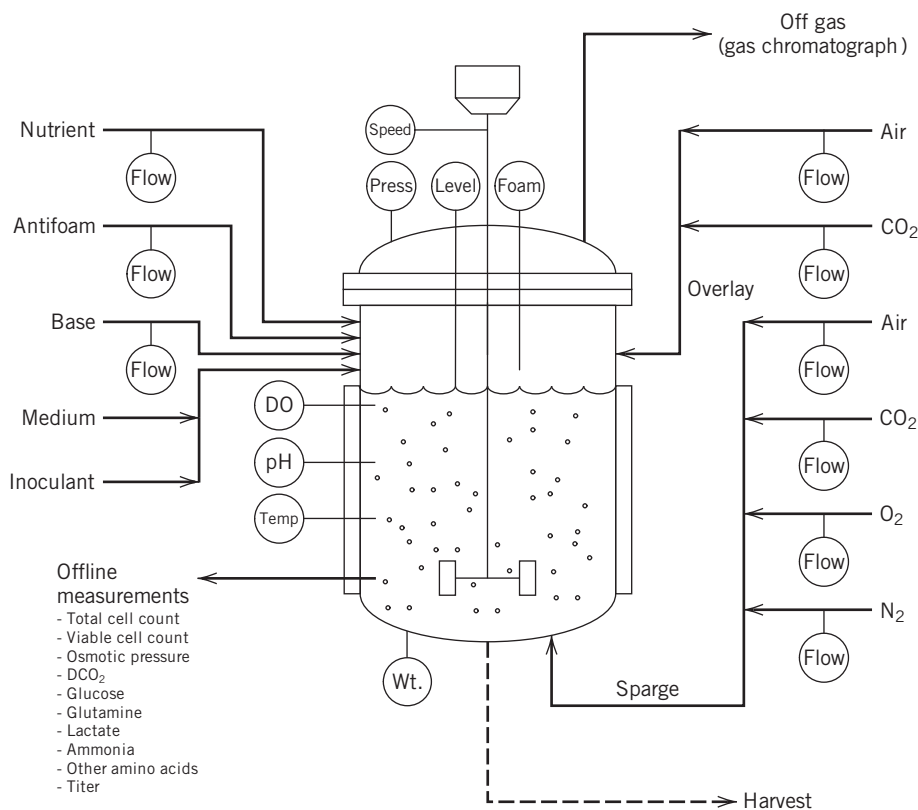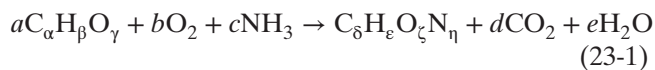
$$a\mathrm{C}_\alpha\mathrm{H}_\beta\mathrm{O}_\gamma + b\mathrm{O}_2 + c\mathrm{NH}_3 \rightarrow \mathrm{C}_\delta\mathrm{H}_\varepsilon\mathrm{O}_\zeta\mathrm{N}_\eta + d\mathrm{CO}_2 + e\mathrm{H}_2\mathrm{O} \tag{23-1}$$

Figure 23.1 Schematic of a typical industrial fermentor. (Figure from Jon Gunther, PhD Thesis, Dept of Chemical Eng., UCSB, 2008).

where $C_\alpha H_\beta O_\gamma$ is the substrate (reactant) and $C_\delta H_\epsilon O_\zeta N_\eta$ is the cell mass (product). For example, in beer making, the substrate is glucose (derived from the wort from grains), and the products are the alcohol and carbon dioxide gas, both of which contribute to the quality of the final product. This apparently straightforward reaction is complicated by the fact that it does not obey simple mass action kinetics; instead, the complex biochemistry underlying the reaction gives rise to unusual nonlinear rate expressions that characterize the enzymatic processes.

Appendix II

A simple dynamic model of a fed-batch bioreactor was given in Chapter 2, Eqs. 2-84 to 2-87. This model can be converted into mass balances on individual components as follows:

Note: CSTR, not fed-batch

$$\frac{dX}{dt} = \mu(S)X - \frac{F}{V}X \qquad (23\text{-}2)$$

$$\frac{dP}{dt} = Y_{P/X}\,\mu(S)X - \frac{F}{V}P \qquad (23\text{-}3)$$

$$\frac{dS}{dt} = \frac{F}{V}(S_f - S) - \mu(S)\frac{X}{Y_{X/S}} \qquad (23\text{-}4)$$

$$\frac{dV}{dt} = F \qquad (23\text{-}5)$$

where the material balance in Eq. 23-2 details the conservation of biomass X, Eq. 23-3 describes the production of metabolites by the cells (biomass), Eq. 23-4 details the conservation of substrate S, and Eq. 23-5 is the overall material balance. The ratio F/V is often denoted as the dilution rate, D. The constants that appear in this equation include the feed concentration of the substrate S_f, the yield of cell mass from substrate $Y_{X/S}$, and the product yield coefficient $Y_{P/X}$. The rate of the biochemical reaction, $\mu(S)$, typically utilizes Monod kinetics given by the saturating function:

An equal sign (=) has been dropped, by typo.

$$\mu(S) \frac{\mu_m S}{K_m + S} \qquad (23\text{-}6)$$

where μ_m is the maximum specific growth rate (limiting value of the rate), and K_m is the substrate saturation constant. Control of this simple reactor involves manipulating the influx of substrate (via the dilution rate, D) to achieve an optimal level of production. More sophisticated control inputs are also possible, including inducers that stimulate the transcription of key genes in the microorganisms, leading to the synthesis of enzymes that maximize product yield.

One of the primary challenges to controlling these reactors in industry is the difficulty in measuring the status of the microorganisms in the fermentor. Specialized sensors (Mandenius, 1994) include enzyme electrodes (e.g., to measure glucose, lactate), calorimetric analyzers (e.g., to measure penicillin), specific gravity (e.g., beer fermentation), and immunosensors (e.g., to measure antigens). However, it remains an open challenge to

develop *in situ* sensors that can monitor a variety of metabolites within the microorganisms in real time.

EXAMPLE 23.1

Consider a fermentor, operated at constant volume, in which a single, rate-limiting substrate promotes biomass growth and product formation. Under the assumption of constant yield, one can derive the following material balances that describe the concentrations in the fermentor (Henson and Seborg, 1991):

A minus sign (-) has been dropped, by typo.

$$\dot{X} = -DX + \mu(S, P)X \qquad (23\text{-}7)$$

$$\dot{S} = D(S_f - S)\frac{1}{Y_{X/S}}\mu(S, P)X \qquad (23\text{-}8)$$

$$\dot{P} = -DP + [\alpha\,\mu(S, P) + \beta]X \qquad (23\text{-}9)$$

For this reactor, the growth term has a more complex shape than the simple Monod expression presented earlier, because both substrate and product can inhibit growth:

$$\mu(S, P) = \frac{\mu_m\left(1 - \dfrac{P}{P_m}\right)S}{K_m + S + S^2/K_i} \qquad (23\text{-}10)$$

The variables X, S, and P are the biomass, substrate, and product concentrations, respectively; D is the manipulated variable (dilution rate); S_f is the feed substrate concentration, and the remaining variables are fixed constants (yield parameters). Take the following values for the fixed parameters:

Table 23.1 Parameter values and units for fermentor in Example 23.1

$Y_{X/S}$	0.4 g/g	α	2.2 g/g
β	0.2 h^{-1}	μ_m	0.48 h^{-1}
P_m	50 g/L	K_m	1.2 g/L
K_i	22 g/L	S_f	20 g/L

(a) Assume a nominal operating point is $D = 0.202$ h^{-1} (dilution rate). The corresponding steady-state or equilibrium values of X, S, and P are 6.0, 5.0, and 19.14 g/L, respectively. Calculate the linearized model at this operating point, and determine the poles, zeros, and steady-state gain.

(b) Simulate the biomass X response to ±10% relative changes in dilution rate.

(c) Next, change the nominal dilution rate to $D = 0.0389$ h^{-1}. The corresponding equilibrium values of X, S, and P are 6.0, 5.0, and 44.05 g/L, respectively. (Does anything look unusual here?). Recalculate the linearized model at this operating point, as well as the poles, zeros, and steady-state gain.

(d) Simulate the biomass response to ±10% relative changes in dilution rate.

(e) Comment on the extreme differences in behavior of the fermentor at these two operating points. What does this indicate about this nonlinear system? What are the implications for control design?

SOLUTION

(a) Using the approach described in Section 4.3, a linearization of the nonlinear model (Eqs. 23-7 through 23-10) is performed. From the resulting model, one can derive a transfer function model with three poles and two zeros. The stable poles are calculated as the complex conjugate pair, $-0.1469 \pm 0.0694j$, and the stable real pole at -0.2020. The zeros are both real and have the values: -0.1631, -0.2020. Finally, the steady-state process gain is -39.54.

(b) The simulated responses are depicted in Fig. 23.2.

(c) As in part (a), the model is linearized, now at the new operating point. The poles are calculated as the complex conjugate pair, $-0.0632 \pm 0.0852j$, and the stable real pole at -0.0389. The zeros are both real and have the values: -0.1630, -0.0389. Notice that one of the zeros is now nonminimum phase. Finally, the steady-state process gain is 86.90, indicating that the sign of the gain has been reversed.

(d) The simulated responses are depicted in Fig. 23.3.

(e) In the first case ($D = 0.202 \ \mathrm{h^{-1}}$), the process gain was negative and the zeros were both negative. In the second case ($D = 0.0389 \ \mathrm{h^{-1}}$), the process gain was positive and one of the zeros becomes nonminimum phase, exhibiting inverse response. This suggests that the fermentor exhibits a dramatic nonlinearity, in which the gain can change sign and process zeros can change from negative to positive (indeed, a plot of the steady-state relationship between the dilution rate and the biomass
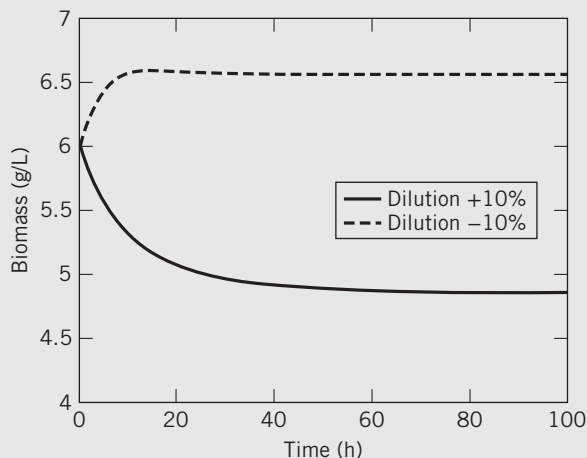

Figure 23.2 Step response of fermentor model to symmetric changes in D of magnitude 10% from the nominal value of $D = 0.202 \ \mathrm{h^{-1}}$.

for this fermentor reveals a parabolic shape; also see Exercise 2.15). This suggests that operation across this gain change requires a nonlinear controller or an adaptive control scheme.
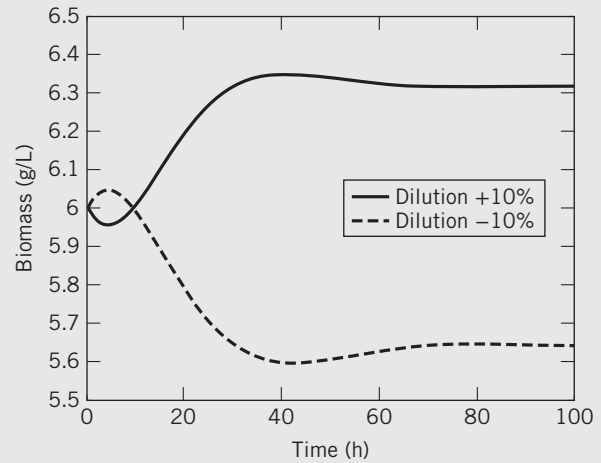

Figure 23.3 Step response of fermentor model to symmetric changes in dilution of magnitude 10% from the nominal value of $D = 0.0389 \ \mathrm{h^{-1}}$.

23.1.2   Crystallizers

The operation of crystallization allows the separation of one phase (in this case, the solid from a solution) so that the product has desirable properties. The solid product that results from crystallization is a highly ordered solid structure, which may have other desirable attributes, including morphology (e.g., shape), that are of direct benefit to the value of the final product. In the pharmaceutical industry, crystal size and shape may facilitate downstream solids processing and/or may be directly related to the final drug formulation, such as bioavailability, shelf life, toxicity, and drug dissolution (Fujiwara et al., 2005; Nagy and Braatz, 2012). Crystallization also finds application in the food industry to improve taste, as well as shelf life, for a diverse range of products (Larsen et al., 2006).

In order to explain the process control strategies employed in the operation of an industrial crystallizer, it is important to review briefly the concept of supersaturation and its relevance to crystallization (Larsen et al., 2006). Saturation refers to the property of phase equilibrium, in this case the equilibrium between the liquid and the dissolved solid (i.e., the solubility of the solid in the liquid). The state of supersaturation refers to the condition in which the liquid solution contains more solid than the amount that corresponds to the solubility (equilibrium), and the system exists in a so-called metastable state. Crystal formation can be induced by changing the operating conditions, such as temperature,

so that the supersaturation state cannot be sustained, and a crystal is nucleated, or created, from the solution. As the dissolved component moves from the solution to the solid crystal phase, the concentration is, of course, lowered. Once a crystal is formed, it continues to grow as a function of the operating temperature and the concentration in the solution. In effect, the operation of crystallization involves the manipulation of this supersaturation state, trading off the formation of new crystals against the growth of existing ones.

An industrial crystallizer is operated typically in a batch mode, so that the management of the supersaturation state is accomplished over the course of the batch cycle time. The available manipulated inputs are the cooling jacket and steam flow rates for temperature management, and the inflow of antisolvent (a component that lowers the solvation capability of the liquid) and solvent, to regulate the concentration of the solution (Zhou et al., 2006). A typical crystallization flowsheet is depicted in Fig. 23.4. Measurement of temperature is straightforward, and there are an increasing number of sophisticated instruments available for measurement of the crystal properties. These include turbidity sensors (to detect the presence of solids), laser scattering instruments (to extract the distribution of crystal sizes in the unit), and spectroscopic instruments, e.g., attenuated total reflectance-Fourier transformed infrared (ATR-FTIR), for measuring solution concentrations (Fujiwara et al., 2005; Larsen et al., 2006; Nagy and Braatz, 2012). More recently, a variety of imaging techniques have been used to measure crystal-shape properties (morphology), such as width and length. As mentioned earlier, these size and shape properties are major determinants for the resulting utility of the product (e.g., drug solubility), and it may be desirable to produce crystals with very uniform properties (i.e., narrow size distribution). Model-based control strategies, for example, optimization-based methods, are being employed to control crystal shape, including polymorphic forms (Nagy and Braatz, 2012).

23.1.3   Granulation

Granulation is a widely used process in which small particles agglomerate into larger granules. In wet granulation processes, the coagulation of particles is improved by the addition of a *binder liquid*, sprayed over an agitated powder in a tumbling drum or pan. The particles are wetted by the binder and a nucleate. The resulting binder-coated granules then collide and stick to form larger granules. These granules can also compact and consolidate as the binder liquid is brought to the surface of the aggregates by stirring in the granulator. Particles can also break because of collisions with the other particles or the granulator walls during mixing. Thus, the main phenomena in granulation processes are granule wetting and nucleation, consolidation and growth, and aggregation and breakage (Mort et al., 2001).

Granulation plays a key role in producing particles with special characteristics, such as time-release attributes (e.g., fertilizer, pharmaceutical tablet). However, in practice, inefficient operation, with very small yields and large recycle ratios (typically 4:1, recycle: product), often occurs. This inefficiency is due to the difficulty in designing and controlling granulation circuits that allow maintenance of specified size ranges for the granules.

As with crystallization, the key challenges for controlling a granulator are to produce particles with desirable attributes, to simplify downstream processing, and to realize end-product properties. In the pharmaceutical industry, granulation is usually accomplished in batch reactors, owing to the relatively small amount of material throughput. The key particle process that must be regulated is the agglomeration of smaller particles into larger particles. Manipulated inputs include binder spray addition (and/or viscosity), particle flow rate, temperature, mixing conditions (including shear), recycle of oversize (crushed) and undersize (fines) particles, and changing the rate of agitation (mixing) in the vessel (Pottmann et al., 2000; Mort et al., 2001; Faure et al., 2001). Some applications also incorporate heating,
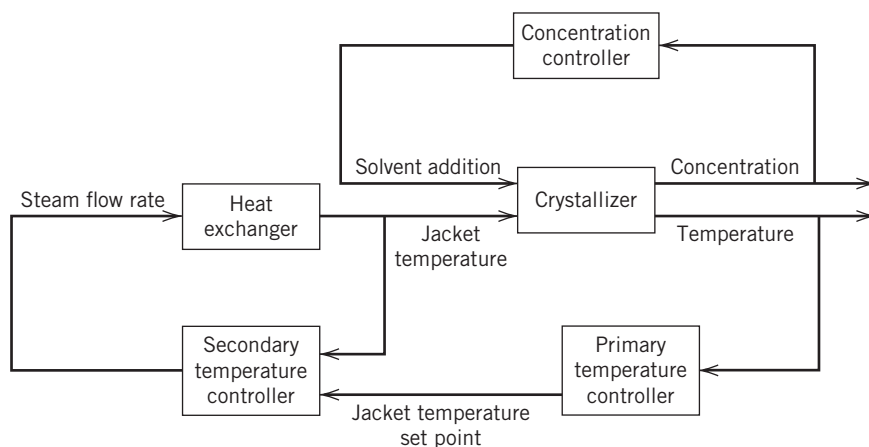

Figure 23.4 Flowsheet of a typical industrial batch crystallizer, showing concentration and temperature controllers, including cascade control for temperature.
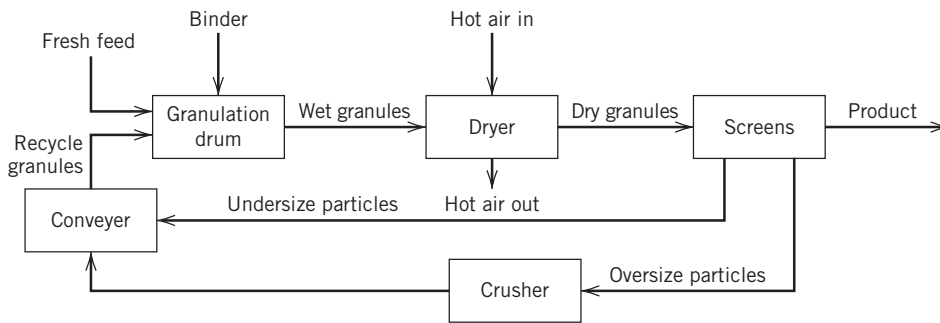
Figure 23.5 Process flowsheet for granulation circuit with recycle.

which introduces temperature control considerations. The measurements currently available are the torque on the agitator (which yields an inference of the load in the vessel and its size and moisture content) and, in more recent installations, measurements of particle size (possibly as a distribution). When a particle size distribution (PSD) is measured (e.g., by imaging methods or laser scattering), it is typically consolidated into one or more scalar measures of the distribution (e.g., the mean size, or d_x, the size of the particle in the *xth* percentile of the distribution (d_5, d_{90}, etc.)).

Process control strategies that utilize these measurements are finding application in wet granulation processes, that is, pharmaceutical industry (Faure et al., 2001), fluid bed granulation (Burggraeve, et al., 2011), and continuous drum granulation processes (Glaser et al., 2009). A typical continuous granulation flowsheet is depicted in Figure 23.5. Batch granulation operation can benefit from traditional monitoring and quality approaches, as detailed in Chapters 21 and 22 (Burggraeve et al., 2011).

and the measured controlled variables are the bulk density and the 5th and 90th percentiles of the particle size distribution (d_5 and d_{90}, respectively). Pottmann et al. (2000) identified a first-order-plus-time-delay model for each combination of inputs and outputs (3×3 problem) with the following parameters (time units are dimensionless):

$$G_{ij}(s) = \frac{K_{ij}}{\tau_{ij}s + 1}e^{-\theta_{ij}s} \tag{23-11}$$

$$K_{ij} = \begin{bmatrix} 0.20 & 0.58 & 0.35 \\ 0.25 & 1.10 & 1.30 \\ 0.30 & 0.70 & 1.20 \end{bmatrix} \tag{23-12}$$

$$\tau_{ij} = \begin{bmatrix} 2 & 2 & 2 \\ 3 & 3 & 3 \\ 4 & 4 & 4 \end{bmatrix} \tag{23-13}$$

$$\theta_{ij} = \begin{bmatrix} 3 & 3 & 3 \\ 3 & 3 & 3 \\ 3 & 3 & 3 \end{bmatrix} \tag{23-14}$$

The units for both the manipulated inputs and the measurements are dimensionless, and the nominal conditions (on which deviation variables are based) are 180 for all three nozzles, 40 for bulk density, 400 for d_5, and 1600 for d_{90}.

(a) Using the relative gain array (RGA), determine the most effective pairings between the inputs and the outputs.

EXAMPLE 23.2

A simplified granulation flowsheet (Pottmann et al., 2000) is shown in Fig. 23.6. The manipulated inputs are the liquid flow rates of binder introduced in three different nozzles,
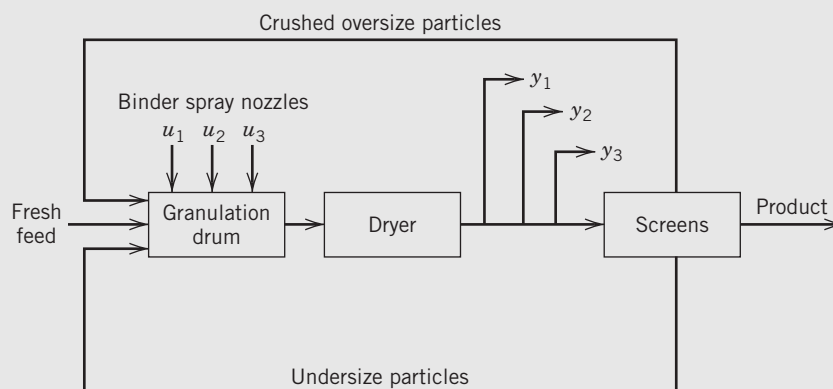

Figure 23.6 Simplified process flowsheet for granulator example. Here u_1, u_2, and u_3 are, respectively, nozzles 1, 2, and 3, and y_1, y_2, and y_3 are, respectively, bulk density, d_5, and d_{90}.

(b) Design three PI + Smith predictor controllers using the IMC design method (see Table 12.1, and assume that a value of $\tau_c = 5$ is employed). Keep in mind that the IMC/PI tuning is for the delay-free part of the plant with a Smith predictor. For the Smith Predictor design, use the method detailed in Chapters 16 and keep in mind that you need to select one delay value for each input–output pair.

(c) Simulate the system response for the three PI + Smith predictor controllers using a step set-point change of [10 0 0]. Be sure to enforce the constraints on the manipulated variables (lower bound of 105; upper bound of 345). Repeat the simulation for a step set-point change of [50 0 0].

SOLUTION

(a) The relative gain array is calculated as detailed in Section 18.2 from the process gains:

$$RGA = K \otimes (K^{-1})^T$$

$$= \begin{bmatrix} 1.0256 & 0.6529 & -0.6785 \\ -1.4103 & 1.8574 & 0.5528 \\ 1.3846 & -1.5103 & 1.1257 \end{bmatrix} \quad (23\text{-}15)$$

Hence, the diagonal pairing of the controllers is recommended (1-1/2-2/3-3), because there are no negative values, and two of the three loops are paired on RGA values very close to 1.

(b) The individual controllers are given calculated from Table 12.1, row A:

Loop 1: $K_c = (2/5)/.2 = 2.0$; $\tau_I = 2$
Loop 2: $K_c = (3/5)/1.1 = 0.545$; $\tau_I = 3$
Loop 3: $K_c = (4/5)/1.2 = 0.667$; $\tau_I = 4$

(c) The simulation results are shown in Figs. 23.7 and 23.8. Note that enforcing the constraints for the second case leads to an unattainable set point for the first output.
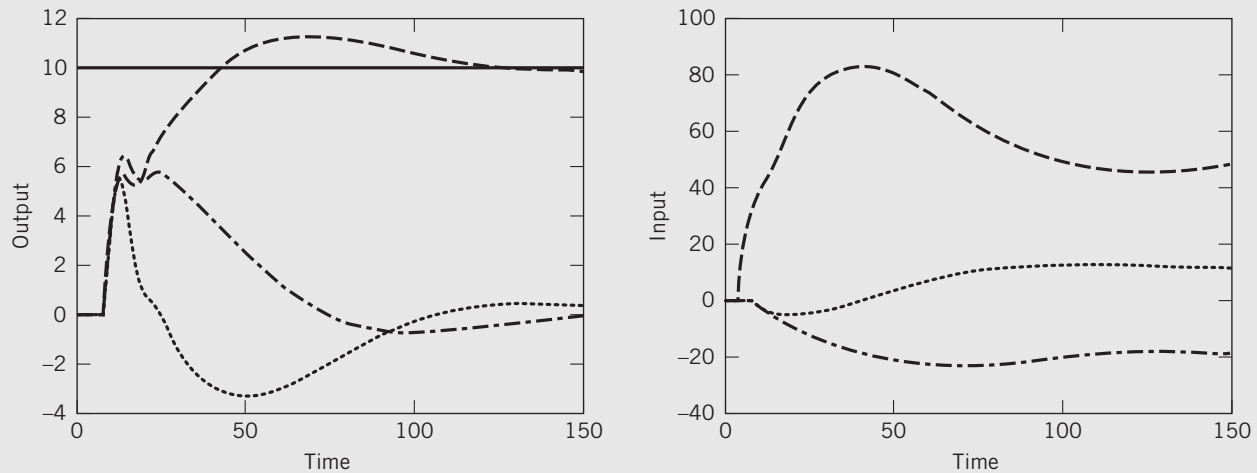

Figure 23.7 Closed-loop response of granulator to +10 step change (introduced at time = 5) in set point for y_1: left plot is CVs, right plot is MVs (----, y_1 and u_1; ------, y_3 and u_3; ...., y_2 and u_2).
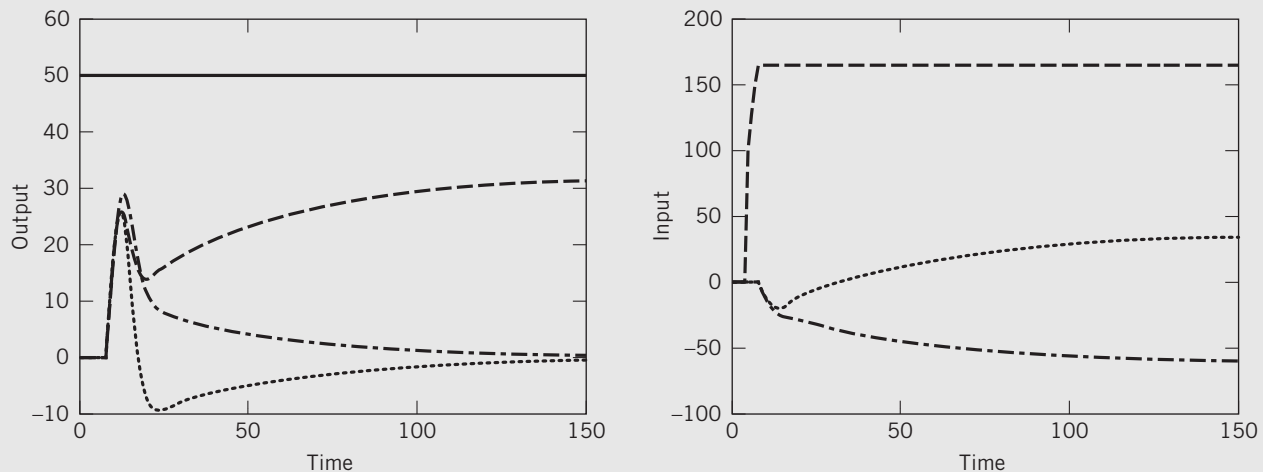

Figure 23.8 Closed-loop response of granulator to +50 step change (introduced at time = 5) in set point for y_1, with constraints enforced on the inputs. The left plot is CVs, right plot is MVs (----, y_1 and u_1; ------, y_3 and u_3; ...., y_2 and u_2).

As indicated in Chapter 22, batch processes can benefit from recipe modifications in between consecutive batches or cycles, using a run-to-run (RtR) strategy. Run-to-run control strategies have also been developed for diabetes control, by considering glucose data for a meal response or an entire day to be the batch of interest. The similarities between the diabetic patient and the batch reactor recipe that motivate the application of this technique are the following:

1. The recipe (24-h cycle) for a human patient consists of a repeated meal protocol (typically three meals), with some variation on meal type, timing, and duration.

2. There is not an accurate dynamic model available to describe the detailed glucose response of each individual to the meal profile.

3. There are selected measurements available that might be used to characterize the quality of the glucose response for a 24-h day, including maximum and minimum glucose values.

Using currently available glucose meters, the blood sampling is very sparse, typically about six to eight measurements per day; hence, the overall quality (i.e., glycemic regulation) has to be inferred from these infrequent samples. The results of a subsequent clinical trial (Zisser et al., 2005) demonstrated that a large fraction of the patients responded favorably to this type of control. Current technology that is available for patients allows the continuous measurement of (subcutaneous) blood sugar with a 5-min sampling period (Harvey et al., 2010). This has enabled a wide array of closed-loop strategies for closed-loop control of insulin pumps, leading to the so-called *artificial pancreas*. From 2004 to 2014, there have been over 40 publications that report closed-loop clinical testing of an artificial pancreas, using PID, MPC, and fuzzy logic-based algorithms (Doyle III et al., 2014).

EXAMPLE 23.3

A patient with Type I diabetes needs an automated scheme to maintain her glucose within an acceptable range, widened here to allow less conservative control (54 mg/dL $< G <$ 144 mg/dL). She has just eaten a large meal (a disturbance) that you estimate will introduce glucose into her bloodstream according to $D(t) = 9.0e^{-0.05t}$, where t is in minutes and $D(t)$ is in mg/dL-min. She has a subcutaneous insulin pump that can release insulin up to 115 mU/min (mU $= 10^{-3}$ Units of insulin). The "U" is a standard convention used to denote the strength of an insulin solution. The flow rate of insulin is the manipulated variable.

A simple model of her blood glucose level is given by Bequette (2002):

$$\frac{dG}{dt} = -p_1 G - X(G + G_{Basal}) + D \qquad (23\text{-}16)$$

$$\frac{dX}{dt} = -p_2 X + p_3 I \qquad (23\text{-}17)$$

$$\frac{dI}{dt} = -n(I + I_{Basal}) + \frac{U}{V_1} \qquad (23\text{-}18)$$

where the constants are defined as follows: $p_1 = 0.028735$ [min^{-1}], $p_2 = 0.028344$ [min^{-1}], $p_3 = 5.035\text{E-}5$ [min^{-1}], $V_1 = 12$ [L], and $n = 0.0926$ [min^{-1}]. G, X, and I are values for glucose concentration (deviation) in the blood (mg/dL), insulin concentration (deviation) at the active site (mU/L), and blood insulin concentration, expressed in deviation variables. Basal values refer to the initial or baseline values for G and I ($G_{Basal} = 81$ mg/dL and $I_{Basal} = 15$ mU/L). D is the rate of glucose release into the blood (mg/dL-min) as the disturbance. U is the flow rate of insulin (mU/min) as the manipulated variable.

(a) What will happen to her blood glucose level if the pump is shut off initially?

(b) What will happen to her blood glucose level if the pump injects insulin at a constant rate of 15 mU/min?

(c) Is there a constant value of U that will help her stay within an acceptable glucose range (54 mg/dL $< G <$ 170 mg/dL) for the next 400 min?

SOLUTION

(a) As shown in Fig. 23.10, the patient's blood glucose will rise in a ramplike fashion if the insulin pump fails (i.e., shuts off). This can also occur as a result of a catheter occlusion (blockage) with the insulin pump.

(b) In this case (Fig. 23.11), the patient's blood sugar peaks, at slightly over 175 mg/dL, and takes 4 h to converge back to a steady-state glucose value of approximately 90 mg/dL.

(c) A setting of 25 mU/min yields the response in Fig. 23.12, which might be deemed too aggressive by many doctors, because of the low post-meal glucose values, motivating a more advanced (i.e., closed-loop) approach to glucose management.
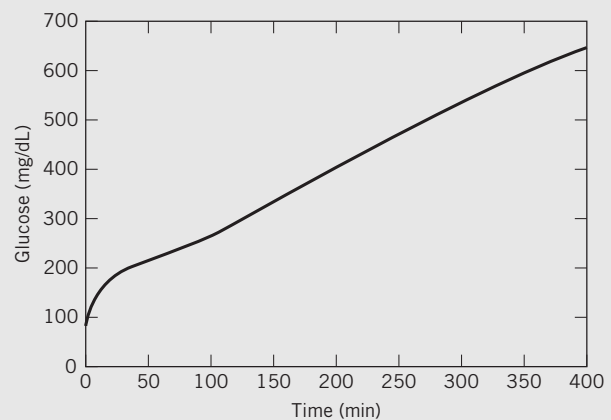

Figure 23.10 Open-loop response of patient's blood glucose when the insulin pump is turned off.
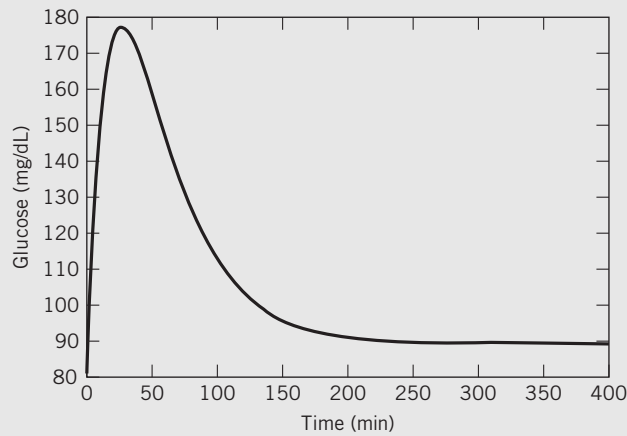
Figure 23.11 Open-loop response of the patient's blood glucose to a constant infusion rate of 15 mU/min from her insulin pump.
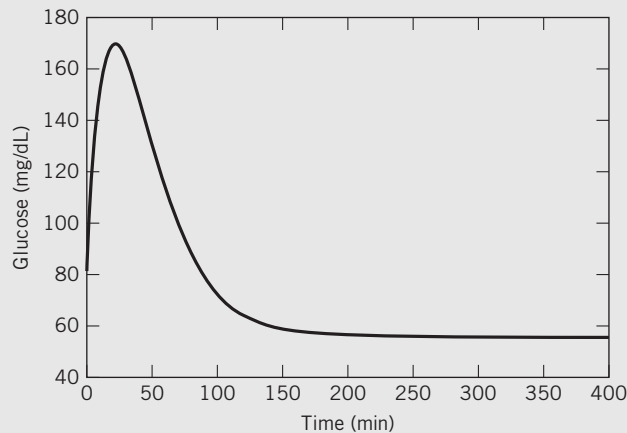

Figure 23.12 Open-loop response of patient's blood glucose to a constant infusion rate of 25 mU/min from her insulin pump.

23.2.2   Blood Pressure Regulation

In both the operating room and postoperative care contexts, closed-loop control of blood pressure and related variables (such as cardiac output and depth of anesthesia) have been studied for a number of years (e.g., Rao et al., 1999; Dumont and Ansermino, 2013), and human clinical trials have proved the efficacy of the approach (Bailey and Haddad, 2005; Araki and Furutani, 2005; Sarabadani et al., 2013). The postoperative application was handled typically by the administration of sodium nitroprusside (SNP) by a nurse via a continuous intravenous (IV) pump. SNP is a vasodilator that achieves blood pressure reduction by relaxing the muscles controlling the vascular resistance to flow through blood vessels. The current technology for both sensors and

infusion pumps is facilitating the design of completely automated control strategies.

The context of the operating room is more complicated, with many critical variables that must be monitored. But an advantage of this setting is that nonportable sensors can be employed that would be too cumbersome or impractical for ambulatory applications. The measured variables include mean arterial pressure (MAP), cardiac output (CO), and depth of anesthesia (DOA). The DOA has been the subject of intense research activity over the last decade, and sensors are available to determine the depth of anesthesia through correlations. These sensors are inferential (see Chapter 16), in that they do not directly measure the medical state of anesthesia, which is characterized by such patient responses as hypnosis, amnesia, analgesia, and muscle relaxation (Araki and Furutani, 2005); rather, they measure the state of electrical activity in the patient's brain. One of the more promising methods is the bispectral index, derived from signal analysis of an electroencephalograph (EEG) (Bailey and Haddad, 2005). A variety of manipulated inputs are also available, resulting in an intrinsically multivariable control problem. Some candidate manipulated variables include vasoactive drugs, such as dopamine and SNP, as well as anesthetics (isoflurane, propofol, etc.).

EXAMPLE 23.4

Consider the following model for predicting the influence of two drugs: SNP, [μg/kg-min]) and dopamine (DPM, [μg/kg-min]), on two medical variables (mean arterial pressure MAP, [mmHg]) and cardiac output CO, [L/(kg-min)]), where time is measured in minutes (Bequette, 2007):

$$\begin{bmatrix} MAP \\ CO \end{bmatrix} = \begin{bmatrix} \dfrac{-6e^{-0.75s}}{0.67s+1} & \dfrac{3e^{-s}}{2.0s+1} \\ \dfrac{12e^{-0.75s}}{0.67s+1} & \dfrac{5e^{-s}}{5.0s+1} \end{bmatrix} \begin{bmatrix} SNP \\ DPM \end{bmatrix} \qquad (23\text{-}19)$$

(a) Calculate the RGA for this problem and propose the appropriate control-loop pairing.

(b) Consider the pairing, SNP-MAP and DPM-CO, as is typically used in practice. Design a pair of PI controllers for this process, using the IMC tuning rules (Table 12.1) and choosing a value of τ_c for each controller that is equal to the corresponding open-loop time constant for that subsystem.

(c) Simulate the closed-loop response to a -10 mmHg change in the MAP set point, while holding CO constant. Discuss the extent of control-loop interactions.

SOLUTION

(a) Using the RGA calculation in Eq. 18-34, $\lambda_{11} = 0.4545$; therefore, the loop pairings apparently should be the 1-2/2-1 pairing, SNP-CO and DPM-MAP.

(b) From Table 12.1, the following values for the PI controller settings are calculated:

Loop 1: $K_c = -(0.67)/(6*(0.67 + .75)) = -0.0786$

$\tau_I = 0.67$

Loop 2: $K_c = (5)/(5*(5 + 1)) = 0.1667$

$\tau_I = 5$

(c) The simulated response for the MAP set point change is depicted in Fig. 23.13, where there is a modest undershoot in the MAP response; however, the interacting nature of the process leads to a large excursion in CO. The control tuning constant τ_c could be refined to trade-off speed versus overshoot and interaction, or by designing a multivariable controller, such as MPC.
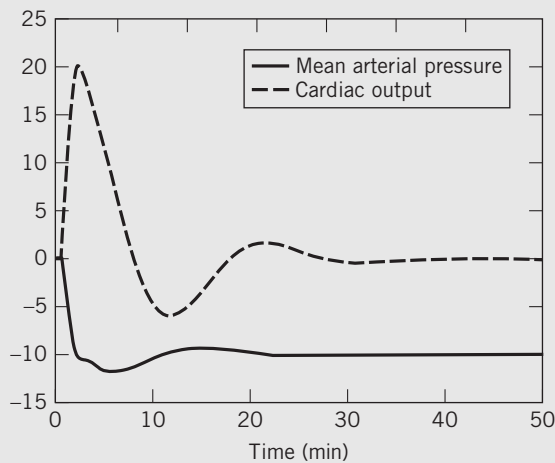

Figure 23.13 Closed-loop response of patient's mean arterial blood pressure and cardiac output to a −10 mmHg change in the MAP set point.

23.2.3 Cancer Treatment

Cancer treatment has changed dramatically over the past decade, in large part enabled by advances in imaging technology. Surgery has been the classical method for attacking cancerous tumors, and more recently X-ray radiation has been employed. An unfortunate side effect in both cases is that healthy tissue can be compromised by inappropriate surgery or delivery of radiation, respectively. Chemotherapy is often be used, alone or in conjunction with surgery or X-ray treatment, and has the advantage that undetected metastases (cancer cells that have circulated through the bloodstream) can be attacked with this method. Thermal therapies (radiofrequency, microwave, or laser techniques) have also been demonstrated to be effective, with similar requirements on targeting the energy to the localized region of the tumor (Dodd et al., 2000). In thermal and radiation treatment, feedback control is finding application to the optimized delivery of the treatment (radiation, heat)

to the targeted area (Salomir et al., 2000; Davison and Hwang, 2003; Ledzewicz and Schättler, 2007; Moonen, 2007). In one feedback-based therapy (Salomir et al., 2000), the heat source power was adjusted based on the deviation of temperature from a target at a particular location in the body, including an integral term, very similar to a PID controller. The desired response was that the temperature should rise quickly to the target without overshoot or oscillations.

Parker (2007) describes a strategy for "model-informed" treatment design for delivery of a chemotherapeutic agent. Using a combination of pharmacokinetic and pharmacodynamic models, predictions can be made about the patient's response (e.g., tumor volume) to the manipulated variables, which in this case could include the drug dosage level and schedule for drug administration. This strategy can be implemented by specifying the time horizon over which the patient's response is monitored and by calculating the optimal drug delivery protocol using the RTO methods of Chapter 19.

More recent developments include chemotherapy using antiangiogenic agents, which deprive the tumor from developing blood cells required for growth (Ledzewicz and Schättler, 2007). In this application, information about the state of the tumor (e.g., the tumor volume, derived from MRI data) is used to control the rate of dosing of the antiangiogenic therapy. More recently, model predictive control designs have been proposed for chemotherapeutic protocols, as an example of a decision support tool, as contrasted with an automation tool (Florian et al., 2008).

23.2.4 Controlled Treatment for HIV/AIDS

To address the global problem of HIV/AIDS, a number of mathematical models and control algorithms have been proposed to help design better treatments for the disease. The drug categories that have been considered include reverse transcriptase inhibitors and protease inhibitors, which affect reproduction of the virus via transcription and production of the virus from infected cells, respectively. The most effective strategies to date have involved a so-called cocktail of multiple drugs, thus attacking the disease in a vector direction (i.e., multiple, simultaneous targets). Measurements are problematic, consisting of relatively slow techniques based on off-line sampling of blood. However, the slow progression of the disease does not warrant real-time measurements, and thus feedback can still be accomplished on this slow time scale.

In their simplest form, mathematical models have been developed that describe the interactions of healthy CD4+ T cells, infected CD4+ T cells, and free viruses in the form of three coupled ordinary differential equations (Craig and Xia, 2005). Such a model can be

the basis of simple model-based feedback strategies for control and can also be extended to generate more complex models suitable for a model predictive control strategy (Zurakowski et al., 2004), including the design of optimal treatment protocols (Pannocchia et al., 2012).

23.2.5 Cardiac-Assist Devices

Cardiac-assist devices are mechanical pumps that provide cardiac output at an appropriate pressure, to allow normal circulation of blood through the patient's body, subject to the changing demands for cardiac output as a function of the patient's state (e.g., level of exercise, emotion, posture, etc.). The ideal device would mimic the body's own mechanisms for maintaining cardiac output at target levels; however, currently available devices are rather primitive in terms of automation, requiring the patient to adjust the set point (Boston et al., 2000). The first such implantable device received approval by the FDA over a decade ago. Research continues on the design of control algorithms for implantable rotary blood pumps, including PID, fuzzy logic, adaptive control, and optimization-based methods (AlOmari et al., 2013).

One of the more interesting aspects of the control design problem for ventricular-assist devices is the placement of the sensors and actuators: there are the issues of susceptibility to infection, as well as anatomical placement (Paden et al., 2000).

23.2.6 Additional Medical Opportunities for Process Control

There are many other challenges in drug therapy, in which an optimized delivery regimen could be calculated using principles of process control and process optimization, e.g., the modeling and control of the anticoagulant drug, heparin (McAvoy, 2007). Another medical application is the treatment of acute neuropatients with brain hypothermia, to lower the intracranial pressure (ICP). A mathematical model can be developed to relate temperature effects with blood flow. The model can then be used to create an automated closed-loop controller (Gaohua and Kimura, 2006) to adjust the coolant temperature (e.g., by using cold-water circulating blankets) in an effort to regulate the ICP. Control design opportunities have been identified for hemodialysis (Javed et al., 2012), mechanical ventilation for respiration (Li and Haddad, 2013), leukemia treatment and vaccination (Laurino et al., 2013) and Parkinsons treatment (Hacısalihzade, 2013).

SUMMARY

Biological and biomedical processes share a great deal in common with the process applications considered in preceding chapters. The latter applications have a characteristic time constant, often exhibit time delays associated with measurements, and typically are multivariable in nature. In contrast, the types of uncertainties in bioprocesses are quite different, owing to the complex nature of biological regulation (see Chapter 24). In addition, there are multiple safety and regulatory issues that are unique to medical closed-loop systems. Process control strategies for several key unit operations in the bioprocess industries (fermentation, crystallization, and granulation) have been described, along with biomedical applications, such as drug delivery for diabetes and blood pressure control and other examples. In Chapter 24, we focus on the molecular scale of biological systems and consider the feedback mechanisms inherent in naturally occurring biophysical networks.

REFERENCES

Alford, J., *Bioprocess Control: Advantages and Challenges*, Proc. Conf. Chemical Process Control, Lake Louise, Alberta, Canada (2006).

AlOmari, A. H., A. V. Savkin, M. Stevens, D. G. Mason, D. L. Timms, R. F. Salamonsen, and N. H. Lovell, Developments in Control Systems for Rotary Left Ventricular Assist Devices for Heart Failure Patients: A Review, *Physiol. Meas.*, **34**, R1 (2013).

American Diabetes Association, Standards of Medical Care in Diabetes—2014, *Diabetes Care*, **37**, S14 (2014).

Araki, M., and E. Furutani, Computer Control of Physiological States of Patients under and after Surgical Operation, *Annu. Rev. Control*, **29**, 229 (2005).

Bequette, B. W., *Process Control*, Prentice-Hall, Upper Saddle River, NJ, 2002.

Bequette, B. W., Modeling and Control of Drug Infusion in Critical Care, *J. Process Control*, **17**, 582 (2007).

Boston, J., M. Simaan, J. Antaki, and Y. Yu, Control Issues in Rotary Heart Assist Devices, *Proc. American Control Conf.*, **3473** (2000).

Boudreau, M. A., and G. K. McMillan, *New Directions in Bioprocess Modeling and Control*, ISA, NC, 2007.

Burggraevea, A., T. Van Den Kerkhofb, M. Hellingsb, J. P. Remonc, C. Vervaetc, and T. De Beer, Batch Statistical Process Control of a Fluid Bed Granulation Process using In-line Spatial Filter Velocimetry and Product Temperature Measurements, *Eur. J. Pharm. Sci.*, **42**, 584 (2011).

Buckland, B. C., The Translation of Scale in Fermentation Processes: The Impact of Computer Process Control, *Nature Biotechnology*, **2**, 875 (1984).

Carson, E., and C. Cobelli, *Modeling Methodology for Physiology and Medicine*, Elsevier, London, 2013.

Craig, I., and X. Xia, Can HIV/AIDS Be Controlled?, *IEEE Control Sys. Mag.*, **25**, 80–83 (2005).

Davison, D. E., and E.-S. Hwang, Automating Radiotherapy Cancer Treatment: Use of Multirate Observer-Based Control, *Proc. American Control Conf.*, **1194** (2003).

DCCT–The Diabetes Control and Complications Trial Research Group, The Effect of Intensive Treatment of Diabetes on the Development and Progression of Long-Term Complications in Insulin-Dependent Diabetes Mellitus, *New Engl. J. Med.*, **329**, 977 (1993).

Dodd, G. D., M. C. Soulen, R. A. Kane, T. Livraghi, W. R. Lees, Y. Yamashita, A. R. Gillams, O. I. Karahan, and H. Rhim, Minimally Invasive Treatment of Malignant Hepatic Tumors: At the Threshold of a Major Breakthrough, *Radiographics*, **20**, 9 (2000).

Doyle III, F. J., L. M. Huyett, J. B. Lee, H. C. Zisser, and E. Dassau, Closed-Loop Artificial Pancreas Systems: Engineering the Algorithms, *Diabetes Care*, **37**, 1191 (2014).

Doyle, F., L. Jovanovič, D. Seborg, R. S. Parker, B. W. Bequette, A. M. Jeffrey, X. Xia, I. K. Craig, and T. J. McAvoy, A Tutorial of Biomedical Process Control, *J. Process Control*, **17**, 571 (2007).

Doyle, F., L. Jovanovič, and D. E. Seborg, Glucose Control Strategies for Treating Type 1 Diabetes Mellitus, *J. Process Control*, **17**, 572 (2007).

Dumont, G., and J. M. Ansermino, Closed-Loop Control of Anesthesia: A Primer for Anesthesiologists, *Anesthesia & Analgesia*, **117**, 1130 (2013).

Faurea, A., P. Yorkb, and R. C. Rowe, Process Control and Scale-up of Pharmaceutical Wet Granulation Processes: A Review, *Eur. J. Pharm. Biopharm.*, **52**, 269 (2001).

Fleet, G. H. (Ed.), *Wine Microbiology and Biotechnology*, Taylor & Francis, London, U.K., 1993.

Florian, J. A., J. L. Eiseman, and R. S. Parker. Nonlinear Model Predictive Control for Dosing Daily Anticancer Agents: A Tamoxifen Treatment of Breast Cancer Case Study, *Comput. Biol. Med.*, **38**, 339 (2008).

Fujiwara, M., Z. K. Nagy, J. W. Chew, and R. D. Braatz, First-Principles and Direct Design Approaches for the Control of Pharmaceutical Crystallization, *J. Process Control*, **15**, 493 (2005).

Gaohua, L., and H. Kimura, A Mathematical Model of Intracranial Pressure Dynamics for Brain Hypothermia Treatment, *J. Theor. Biol.*, **238**, 882 (2006).

Gatzke, E. P., and F. J. Doyle III, Model Predictive Control of a Granulation System Using Soft Output Constraints and Prioritized Control Objectives, *Powder Tech.*, **121**, 149 (2001).

Glaser, T., C. F. W. Sanders, F. Y. Wang, I. T. Cameron, R. Ramachandran, J. D. Litster, J. M. H. Poon, C. D. Immanuel, and F. J. Doyle III, Model Predictive Control of Drum Granulation, *J. Process Contr.*, **19**, 615 (2009).

Hacısalihzade, S. S., *Biomedical Applications of Control Engineering*, Springer, 2013.

Hahn, J., T. Edison, and T. F. Edgar, Adaptive IMC Control for Drug Infusion for Biological Systems, *Control Eng. Practice*, **10**, 45 (2002).

Harvey, R., Y. Wang, B. Grosman, M. W. Percival, W. Bevier, D. A. Finan, H. Zisser, D. E. Seborg, L. Jovanovic, F. J. Doyle III, and E. Dassau, Quest for the Artificial Pancreas, *IEEE Eng. Med. Biol. Mag.*, **March/April**, 53 (2010).

Heller, A., Integrated Medical Feedback Systems for Drug Delivery, *AIChE J.*, **51**, 1054 (2005).

Henson, M. A., and D. E. Seborg, An Internal Model Control Strategy for Nonlinear Systems, *AIChE J.*, **37**, 1065 (1991).

Javed, F., A. V. Savkin, G. S. H. Chan, J. D. Mackie, and N. H. Lovell, Recent Advances in the Monitoring and Control of Haemodynamic Variables during Haemodialysis: A Review, *Physiol. Meas.*, **33**, R1 (2012).

Jovanovič, L., The Role of Continuous Glucose Monitoring in Gestational Diabetes Mellitus, *Diabetes Technol. Ther.*, **2**, S67 (2000).

Larsen, P. A., D. B. Patience, and J. B. Rawlings, Industrial Crystallization Process Control, *IEEE Control Systems*, **26**, 70 (2006).

Laurino, M., M. Stano, M. Betta, G. Pannocchia, and A. Landi, Combining Pharmacological Therapy and Vaccination in Chronic Myeloid Leukemia via Model Predictive Control, *Proc. IEEE EMBS Conf.*, 3925 (2013).

Ledzewicz, U., and H. Schättler, Antiangiogenic Therapy in Cancer Treatment as an Optimal Control Problem, *SIAM J. Control Optim.*, **46**, 1052 (2007).

Li, H., and W. H. Haddad, Model Predictive Control for a Multicomponent Respiratory, *IEEE Trans. Control Sys. Tech.*, **21**, 1988 (2013).

Mahadevan, R., S. K. Agrawal, and F. J. Doyle III, Differential Flatness Based Nonlinear Predictive Control of Fed-Batch Bioreactors, *Control Eng. Prac.*, **9**, 889 (2001).

Mandenius, C.-F., Process Control in the Bioindustry, *Chemistry Today*, **19**, 19–22 (1994).

Mascia, S., P. L. Heider, H. Zhang, R. Lakerveld, B. Benyahia, P. I. Barton, R. D. Braatz, C. L. Cooney, J. M. B. Evans, T. F. Jamison, K. F. Jensen, A. S. Myerson, and B. L. Trout, End-to-End Continuous Manufacturing of Pharmaceuticals: Integrated Synthesis, Purification, and Final Dosage Formation, *Angew. Chem.*, **52**, 12359 (2013).

McAvoy, T. J., Modeling and Control of the Anticoagulant Drug Heparin, *J. Process Control*, **17**, 590 (2007).

Moonen, C. T. W., Spatio-Temporal Control of Gene Expression and Cancer Treatment Using Magnetic Resonance Imaging-Guided Focused Ultrasound, *Clin. Cancer Res.*, **13**, 3482 (2007).

Morari, M., and A. Gentilini, Challenges and Opportunities in Process Control: Biomedical Processes, *AIChE J.*, **47**, 2140 (2001).

Mort, P. R., S. W. Capeci, and J. W. Holder, Control of Agglomeration Attributes in a Continuous Binder-Agglomeration Process, *Powder Tech.*, **117**, 173 (2001).

Nagy, Z. K., and R. D. Braatz, Advances and New Directions in Crystallization Control, *Annu. Rev. Chem. Biomol. Eng.*, **3**, 55 (2012).

O. de Sa, D., Applied Technology and Instrumentation for Process Control, CRC Press, New York, 2004.

Paden, B., J. Ghosh, and J. Antaki, Control System Architectures for Mechanical Cardiac Assist Devices, *Proc. American Control Conf.*, 3478 (2000).

Pannocchia, G., Laurino, M., and A. Landi, A Model Predictive Control Strategy Toward Optimal Structured Treatment Interruptions in Anti-HIV Therapy, *IEEE Trans. Biomed. Eng.*, **57**, 1040 (2012).

Parker, R. S., Modeling for Anti-Cancer Chemotherapy Design, *J. Process Control*, **17**, 576 (2007).

Pottmann, M., B. A. Ogunnaike, A. A. Adetayo, and B. J. Ennis, Model-Based Control of a Granulation System, *Powder Tech.*, **108**, 192 (2000).

Rao, R. R., J. W. Huang, B. W. Bequette, H. Kaufman, and R. J. Roy, Control of a Nonsquare Drug Infusion System: A Simulation Study, *Biotechnol. Prog.*, **15**, 556 (1999).

Rohani, S., M. Haeri, and H. C. Wood, Modeling and Control of a Continuous Crystallization Process Part 1. Linear and Non-Linear Modeling, *Comput. Chem. Eng.*, **23**, 263 (1999).

Salomir, R., F. C. Vimeux, J. A. de Zwart, N. Grenier, and C. T. W. Moonen, Hyperthermia by MR-Guided Focused Ultrasound: Accurate Temperature Control Based on Fast MRI and a Physical Model of Local Energy Deposition and Heat Conduction, *Magnetic Resonance in Medicine*, **43**, 342 (2000).

Sarabadani, A., S. Bernasconi, V. Klamroth-Marganska, S. Nussbaumer, and R. Riener, Model-free Predictive Control of Human Heart Rate and Blood Pressure, *Proc. IEEE Intl. Conf. Bioinformatics and Bioengineering*, **1**, (2013).

Schügerl, K., Progress in Monitoring, Modeling and Control of Bioprocesses during the Last 20 Years, *J. Biotechnol.*, **85**, 149 (2001).

Sheldon, R. A., The E Factor: Fifteen Years On, *Green Chem.*, **9**, 1273 (2007).

Steil, G. M., K. Rebrin, C. Darwin, F. Hariri, and M. F. Saad, Feasibility of Automating Insulin Delivery for the Treatment of Type 1 Diabetes, *Diabetes*, **55**, 3344 (2006).

Van Impe, J. F., P. A. Vanrolleghem, and D. M. Iserentant, *Advanced Instrumentation, Data Interpretation, and Control of Biotechnological Processes*, Kluwer, Dordrecht, 1998.

Zisser, H., L. Jovanovič, F. Doyle III, P. Ospina, and C. Owens, Run-to-Run Control of Meal-Related Insulin Dosing, *Diabetes Technol. Ther.*, **7**, 48 (2005).

Zhou, G. X., M. Fujiwara, X. Y. Woo, E. Rusli, H.-H. Tung, C. Starbuck, O. Davidson, Z. Ge, and R. D. Braatz, Direct Design of Pharmaceutical Antisolvent Crystallization through Concentration Control, *Crystal Growth & Design*, **6**, 892 (2006).

Zurakowski, R., M. J. Messina, S. E. Tuna, and A. R. Teel, HIV Treatment Scheduling Via Robust Nonlinear Model Predictive Control, *Proc. Asian Control Conf.*, **25** (2004).

EXERCISES

23.1 Consider the fermentor problem in Example 23.1.
(a) Design an IMC controller for the first operating point (dilution = 0.202 h^{-1}), and simulate the response to both a +0.5 [g/L] and a −0.5 [g/L] change in the biomass concentration set point. Then, simulate the response to both a +1 [g/L] and a −1 [g/L] change in the biomass concentration set point.

(b) Simulate the response of a −12.5% step change in the maximum growth rate (μ_m). How well does the controller perform?

(c) Comment on the observed nonlinearity in the system.

(d) Discuss how the controller design would change if there were a requirement to operate at the lower dilution operating point. What do you need to consider in this case?

23.2 Consider the granulation model that was given in Example 23.2.
(a) Design an MPC controller, using the nominal process model. Initially consider a control horizon of $M = 2$ and a prediction horizon of $P = 40$ (with a sampling period of $\Delta t = 1$). Use equal weights on the manipulated inputs and penalize the two percentile outputs equally, but use a larger weight on the bulk density y_1.

(b) Consider the effect of a plant-model mismatch. Use the problem statement for control design, but assume that the actual process is characterized by the following parameters:

$$\widehat{K}_{i,j} = \begin{bmatrix} 0.10 & 0.90 & 0.15 \\ 0.25 & 1.10 & 1.30 \\ 0.50 & 0.80 & 1.00 \end{bmatrix}$$

$$\widehat{\tau}_{i,j} = \begin{bmatrix} 1 & 2 & 1.5 \\ 3 & 3 & 3 \\ 3 & 3 & 3 \end{bmatrix}$$

$$\widehat{\theta}_{i,j} = \begin{bmatrix} 2 & 2 & 4 \\ 2 & 3 & 4 \\ 2 & 3 & 4 \end{bmatrix}$$

(c) These models are in deviation variables, but the actual steady-state flow rates for the nozzles are 175, 175, and 245, respectively. The steady-state outputs are 40, 400, and 1620, respectively. Nozzle flow rates are limited to values between 100 and 340, and it is desired to keep the 5th percentile (y_2)

above 350 and the 90th percentile y_3 below 1650. Simulate the response of the controller to the following changes:

(i) Step change in bulk density from 40 to 90.

(ii) Simultaneous change in the 5th percentile from 400 to 375 and 90th percentile from 1620 to 1630.

Comment on the performance of your controller (and retune as necessary).

23.3 Gaohua and Kimura (2006) derived an empirical patient model for the manipulation of ambient temperature u (°C) to influence the patient's brain intracranial pressure (ICP) y (mm Hg). The medical data support the following empirical values for a first-order-plus-time-delay model to describe the effect of cooling temperature (°C) on the ICP (mmHg) in time units of hours:

$$G(s) = \frac{4.7}{9.6s + 1} e^{-s}$$

The nominal values for the process variables are: ICP = 20 mmHg; ambient temperature = 30 °C.

(a) Using the IMC tuning rules, derive an appropriate PI controller for this medical experiment. (*Hint*: begin with a value τ_c =1.0 h). What does that value of τ_c mean?

(b) Simulate the response of a 10-mmHg reduction in ICP. What is the overshoot? What is the minimum value of the temperature? What is the settling time?

(c) Comment on whether this is a reasonable controller design for a biomedical application. How might you improve the design?

23.4 In a rehabilitation training experiment for a neurological patient, a step change in treadmill speed of +2.5 km/h was made. The patient heart rate response HR is given in Fig. E23.4.
(a) Derive an appropriate first-order-plus-time-delay model for the patient dynamics.

(b) The doctors wish to control the patient's heart rate to a nearly constant value by adjusting treadmill speed. Using the IMC tuning rules, design a suitable PI controller for this patient. Simulate the response of the controller for a step change in the HR of +10 bpm. Calculate the settling time, overshoot, and rise time for the controller. Do these values seem reasonable for a medical application?

(c) How would you improve the procedure for fitting the patient's initial dynamics?
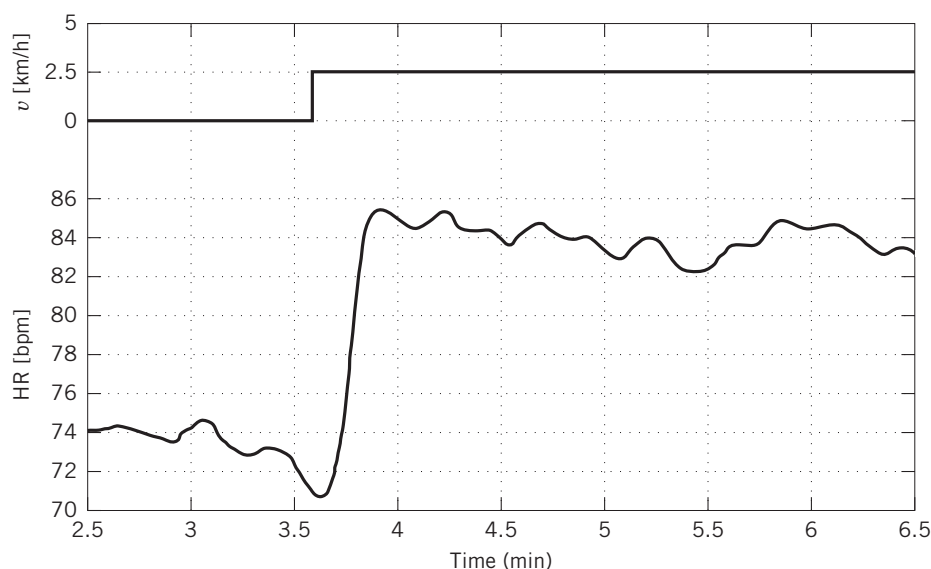
Figure E23.4

23.5 A crystallizer is used to separate a pharmaceutical product from the fermentation extract. The three manipulated variables are the fines dissolution rate u_1, the crystallizer temperature u_2, and the flow rate in the overflow u_3. The nominal values of these three inputs are 2.25×10^{-6} m³/s, 310 K, and 1.5×10^{-6} m³/s, respectively. The three variables to be controlled are the crystal size distribution, as calculated by the fines suspension density y_1; the crystal purity, as calculated by supersaturation conditions y_2; and the product rate y_3. The nominal values of these three inputs are 0.55 K, 11.23 K, and 0.12 kg/kg H_2O, respectively. These variables have multiple interactions, and the following model has been identified from experimental data for a continuous crystallizer, where time is measured in s (Rohani et al., 1999):

$$
\begin{bmatrix} y_1 \\ y_2 \\ y_3 \end{bmatrix} = \begin{bmatrix} \dfrac{72,600}{s + 0.2692} & \dfrac{0.025082(s - 20.0)(s - 10.4)}{s^2 + 10.11s + 96.57} & \dfrac{125,000(s - 1.25)}{s + 0.39} \\[3mm] \dfrac{568,000}{s + 2.11} & \dfrac{-0.15095}{s + 0.1338} & \dfrac{-1,830,000(s + 0.089)}{s + 0.43} \\[3mm] \dfrac{-1870}{s + 0.21} & \dfrac{-0.0071}{s + 0.235} & \dfrac{16,875}{s + 0.2696} \end{bmatrix} \begin{bmatrix} u_1 \\ u_2 \\ u_3 \end{bmatrix}
$$

(a) Calculate the RGA, and determine the appropriate pairings for SISO feedback control. Comment on the role of dynamics in your decision.

(b) Using the IMC tuning rules, design three PI controllers for this process.

(c) Simulate the process response to a step set point, separately, in each of the controlled outputs [use a magnitude of +10% (relative) change]. Next, simulate the response of the system to a simultaneous pair of step changes (again, use a magnitude of +10% relative) in each of the second (purity) and third (product rate) controlled outputs. Try to tune the controller to improve the transient response to the simultaneous step changes.

23.6 Consider the diabetic patient in Example 23.3. Your goal is to design an automated device to administer insulin infusion in response to meal disturbances.

(a) Considering only the insulin-glucose dynamics, calculate an approximate second-order patient model by fitting the responses (changes in insulin) obtained from simulations of the equations given in the example.

(b) Using the IMC tuning rules, design a PID controller for this process.

(c) Simulate the closed-loop system response to a step set point change in blood glucose of −20 mg/dl. Try to tune the controller to improve the transient response.

(d) Simulate the closed-loop system response to the meal disturbance described in Example 23.3. Is the controller able to maintain the safety boundaries for blood glucose (54 mg/dL < G < 144 mg/dL)?

(e) In practice, sensors are available for measuring blood glucose sample from the subcutaneous tissue (the layer of fat under the skin, as opposed to directly from the blood stream). Assuming that such a procedure introduces a pure time delay, repeat the simulation from part (d) with a 10-min sensor delay. How has the performance changed? What is the maximum time delay that the closed-loop design will tolerate before it becomes unstable?

23.7 Recall the artificial pancreas control problem from Section 23.2. In order to regulate blood glucose BG, you have two possible manipulated variables to choose from: pumping insulin F_I and pumping glucagon F_G. As you already learned, insulin can be a life-saving drug, but an overdose of insulin can send the body into a coma. Glucagon operates by converting glycogen in the liver to glucose. Their corresponding transfer functions are given below (time is in minutes):

$$G_{p1}(s) = \frac{BG(s)}{F_I(s)} = \frac{-1.5e^{-30s}}{(20s + 1)(25s + 1)}$$

$$G_{p2}(s) = \frac{BG(s)}{F_G(s)} = \frac{3.4e^{-15s}}{15s + 1}$$

In addition, you have the following information relating the BG to a meal (disturbance) D:

$$G_d(s) = \frac{BG(s)}{D(s)} = \frac{5e^{-10s}}{30s + 1}$$

(a) Using principles you have learned about processes in general, which manipulated variable would you select (insulin pump or glucagon pump) for the design of a feedback control device? Be very specific.

(b) For the insulin pump, design an appropriate PID controller for the system, using IMC tuning rules (assuming $\tau_c = 20$ min).

(c) Derive the theoretically optimal feedforward controller for this device, assuming you use insulin as the MV. Is this controller realizable? (explain why or why not) If not, what might you do to implement an appropriate controller?

(d) For the insulin pump controller you designed above, you are now asked to design a control system for the *pump subsystem only*. Of particular concern is the situation where the pump is not delivering insulin because of an occluded tube. Draw a block diagram for the loop consisting of the pump and a flow controller. Include a type 4 alarm system for safety (See Chapter 10).

23.8 Data from an actual clinical trial for the closed-loop artificial pancreas is summarized in the following cumulative histograms, where the percentage of blood glucose measurements below a particular value is plotted against the blood glucose value. The three curves denote: (i) actual blood glucose BG measurements collected from finger stick measurements (solid), (ii) one continuous glucose measurement sensor CGM2 (dashed), and (iii) a (redundant) second glucose measurement sensor CGM2 (dotted).
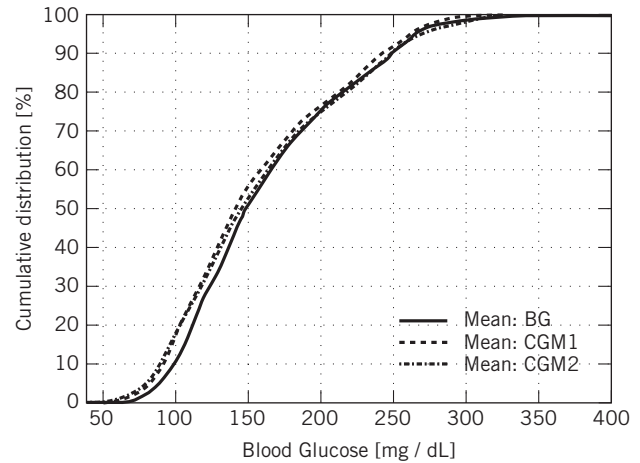
Figure E23.8

From a medical *safety* perspective, one would like to keep the blood glucose measurements in the range of 70–180 mg/dL.

(a) For each of the three measurements (two CGMs and actual BG), compute the fraction of the data that lies in the range 70–180 mg/dL. Comment on the absolute and relative safety of an algorithm that uses these measurements.

(b) Repeat the calculations for the more stringent performance range of 80–140 mg/dL.

(c) Using the concepts introduce in Chapter 9, comment on the error characteristics of the two sensors, using the nomenclature introduced in Section 9.4.3.

$K = G/L$ (the gas-to-liquid ratio), the following model is obtained for the three-stage absorber:

$$\tau\frac{dx_1}{dt} = K(y_f - b) - (1 + \mathcal{S})x_1 + x_2 \tag{2-73}$$

$$\tau\frac{dx_2}{dt} = \mathcal{S}x_1 - (1 + \mathcal{S})x_2 + x_3 \tag{2-74}$$

$$\tau\frac{dx_3}{dt} = \mathcal{S}x_2 - (1 + \mathcal{S})x_3 + x_f \tag{2-75}$$

In the model of Eqs. 2-73 to 2-75, note that the individual equations are linear but also coupled, meaning that each output variable—x_1, x_2, x_3—appears in more than one equation. This feature can make it difficult to convert these three equations into a single higher-order equation in one of the outputs, as was done in Eq. 2-49.

2.4.8 Fed-Batch Bioreactor

Biological reactions that involve microorganisms and enzyme catalysts are pervasive and play a crucial role in the natural world. Without such bioreactions, plant and animal life, as we know it, simply could not exist. Bioreactions also provide the basis for production of a wide variety of pharmaceuticals and healthcare and food products. Other important industrial processes that involve bioreactions include fermentation and wastewater treatment. Chemical engineers are heavily involved with biochemical and biomedical processes. In this section we present a dynamic model for a representative process, a bioreactor operated in a semi-batch mode. Additional biochemical and biomedical applications appear in other chapters.

In general, bioreactions are characterized by the conversion of feed material (or *substrate*) into products and cell mass (or *biomass*). The reactions are typically catalyzed by enzymes (Bailey and Ollis, 1986; Fogler, 2006). When the objective is to produce cells, a small amount of cells (*inoculum*) is added to initiate subsequent cell growth. A broad class of bioreactions can be represented in simplified form as

$$\text{cells} + \text{substrate} \rightarrow \text{more cells} + \text{products} \tag{2-76}$$
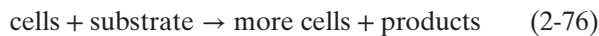
The stoichiometry of bioreactions can be very complex and depends on many factors that include the environmental conditions in the vicinity of the cells. For simplicity we consider the class of bioreactions where the substrate contains a single limiting nutrient and only one product results. The following *yield coefficients* are based on the reaction stoichiometry:

$$Y_{X/S} = \frac{\text{mass of new cells formed}}{\text{mass of substrate consumed to form new cells}} \tag{2-77}$$

$$Y_{P/S} = \frac{\text{mass of product formed}}{\text{mass of substrate consumed to form product}} \tag{2-78}$$

$$Y_{P/X} = \frac{\text{mass of product formed}}{\text{mass of new cells formed}} \tag{2-79}$$

Many important bioreactors are operated in a semi-continuous manner that is referred to as *fed-batch* operation, which is illustrated in Fig. 2.11. A feed stream containing substrate is introduced to the fed-batch reactor continually. The mass flow rate is denoted by F and the substrate mass concentration by S_f. Because there is no exit stream, the volume V of the bioreactor contents increases during the batch. The advantage of fed-batch operation is that it allows the substrate concentration to be maintained at a desired level, in contrast to batch reactors where the substrate concentration varies continually throughout the batch (Shuler and Kargi, 2002).

Fed-batch operation is used to manufacture many important industrial products, including antibiotics and protein pharmaceuticals (Chapter 23). In batch and fed-batch reactors, cell growth occurs in different stages after the inoculum is introduced. We will consider only the exponential growth stage where the cell growth rate is autocatalytic and is assumed to be proportional to the cell concentration. A standard reaction rate expression to describe the rate of cell growth with a single limiting substrate is given by (Bailey and Ollis, 1986; Fogler, 2006)

$$r_g = \mu X \tag{2-80}$$

where r_g is the rate of cell growth per unit volume, X is the cell mass, and μ is the *specific growth rate*, which is well described by the *Monod equation*:

$$\mu = \mu_{max}\frac{S}{K_S + S} \tag{2-81}$$

Note that μ has units of reciprocal time—for example, h^{-1}. Model parameter μ_{max} is referred to as the *maximum growth rate*, because μ has a maximum value of μ_{max} when $S \gg K_S$. The second model parameter, K_S, is called the *Monod constant*. The Monod equation has the same form as the Michaelis–Menten equation, a standard rate expression for enzyme reactions (Bailey and Ollis, 1986; Fogler, 2006). More complex versions of the
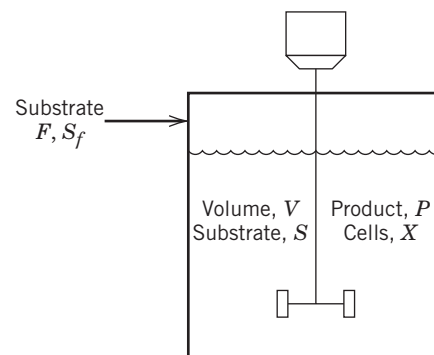

Figure 2.11 Fed-batch reactor for a bioreaction.

specific growth rate are possible including, for example, product inhibition.

A dynamic model for the fed-batch bioreactor in Fig. 2.11 will be derived based on the following assumptions:

1. The cells are growing exponentially.
2. The fed-batch reactor is perfectly mixed.
3. Heat effects are small so that isothermal reactor operation can be assumed.
4. The liquid density is constant.
5. The *broth* in the bioreactor consists of liquid plus solid material (i.e., cell mass). This heterogeneous mixture can be approximated as a homogeneous liquid.
6. The rate of cell growth r_g is given by Eqs. 2-80 and 2-81.
7. The rate of product formation per unit volume r_p can be expressed as

$$r_P = Y_{P/X} r_g \qquad (2\text{-}82)$$

8. The feed stream is sterile and thus contains no cells.

The dynamic model of the fed-batch reactor consists of individual balances for substrate, cell mass, and product, plus an overall mass balance. The general form of each balance is

$$\{Rate\ of\ accumulation\} = \{rate\ in\} + \{rate\ of\ formation\} \qquad (2\text{-}83)$$

The individual component balances are

$$Cells\text{:} \quad \frac{d(XV)}{dt} = Vr_g \qquad (2\text{-}84)$$

$$Product\text{:} \quad \frac{d(PV)}{dt} = Vr_p \qquad (2\text{-}85)$$

$$Substrate\text{:} \quad \frac{d(SV)}{dt} = FS_f - \frac{1}{Y_{X/S}}Vr_g - \frac{1}{Y_{P/S}}Vr_p \qquad (2\text{-}86)$$

where P is the mass concentration of the product and V is reactor volume. Reaction rates r_g and r_p and yield coefficients were defined in Eqs. 2-77 through 2-82. The overall mass balance (assuming constant density) is

$$Mass\text{:} \quad \frac{dV}{dt} = F \qquad (2\text{-}87)$$

The dynamic model is simulated for two different feed rates (0.02 and 0.05 L/h). Figure 2.12 shows the profile of cell, product, and substrate concentration, together with liquid volume in the reactor. The model parameters and
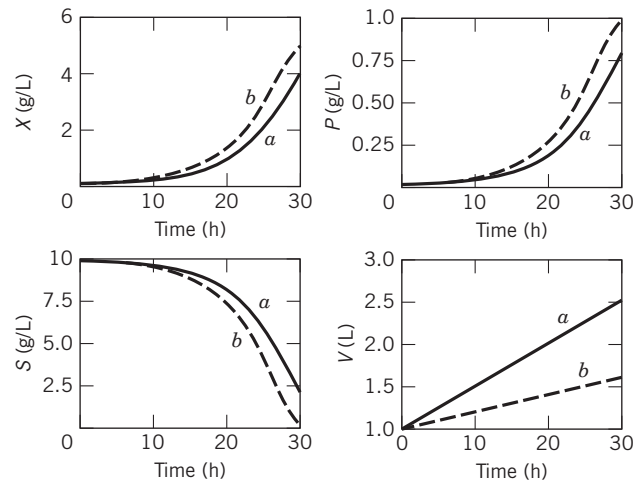

Figure 2.12 Fed-batch reaction profile (a (solid): $F = 0.05$ L/h; b (dashed): $F = 0.02$ L/h).

Table 2.4 Model Parameters and Simulation Conditions for Bioreactor

Model Parameters			Simulation Conditions		
$\mu_{\max}$	0.20	h^{-1}	S_f	10.0	g/L
K_S	1.0	g/L	$X(0)$	0.05	g/L
$Y_{X/S}$	0.5	g/g	$S(0)$	10.0	g/L
$Y_{P/X}$	0.2	g/g	$P(0)$	0.0	g/L
			$V(0)$	1.0	L

simulation conditions are given in Table 2.4. For different feed rates, the bioreactor gives different responses; thus, the product can be maximized by varying F.

2.5 PROCESS DYNAMICS AND MATHEMATICAL MODELS

Once a dynamic model has been developed, it can be solved for a variety of conditions that include changes in the input variables or variations in the model parameters. The transient responses of the output variables as functions of time are calculated by numerical integration after specifying the initial conditions, the inputs and the time interval at which the system is to be integrated.

A large number of numerical integration techniques are available, ranging from simple techniques (e.g., the Euler and Runge–Kutta methods) to more complicated ones (e.g., the implicit Euler and Gear methods). All of these techniques represent some compromise between computational effort (computing time) and accuracy. Although a dynamic model can always be solved in

Short Tutorial on Matlab

(©2004 by Tomas Co)

Part 5. Using S-function blocks in Simulink®

I.   **Motivation:** With the complexity of medium-size to large-size nonlinear models, it may be more efficient to use a set of differential equations written in an m-file. These m-files will be accessed by Simulink through the S-function block. Thus, this method mixes the advantages of an m-file which can be run directly by solvers such as **ode45**, with the graphical links to other Simulink blocks.

II. **Example System:**

Suppose we want to model the nonisothermal CSTR,

$$\frac{dC_a}{dt} = \left(\frac{F}{V}\right) \cdot \left(C_{af} - C_a\right) - k_0 \cdot \exp\left[-\frac{E_a}{R \cdot (T + 460)}\right] \cdot C_a$$

$$\frac{dT}{dt} = \left(\frac{F}{V}\right) \cdot \left(T_f - T\right) - \frac{\Delta H}{\rho \cdot C_p} \cdot \left[k_0 \cdot \exp\left[-\frac{E_a}{R \cdot (T + 460)}\right] \cdot C_a\right] - \left(\frac{U \cdot A}{\rho \cdot C_p \cdot V}\right) \cdot \left(T - T_j\right)$$

We want to model this system in which we will treat the jacket temperature, T_j, as the input (i.e. manipulated variable). We will also want to monitor concentration and temperature of the liquid in the CSTR as our outputs.

III. **Write the m-file.**

Recall that we could model the process by writing an m-file to be used by Matlab solvers such as **ode45**. One such file, which we will name as **reactor.m**, is shown in Figure 1.

Test the model to make sure it works. For instance, with T_j=55 :

```
>> [t,x]=ode45(@reactor,[0 10],[0.1;40],[],55);
```

Note/Recall: The command-line specifies: a simulation-time span of **[0 10]**, an initial-value column vector: **[0.1;40]**, a null placeholder, **[]** , for default options, and setting T_j with a value equal to 55.

```
function    dx = reactor(t,x,Tj)
%
%    model for reactor
%

    Ca   = x(1)            ;    % lbmol/ft^3
    T    = x(2)            ;    % oF

    Ea   = 32400           ;    % BTU/lbmol
    k0   = 15e12           ;    % hr^-1
    dH   = -45000          ;    % BTU/lbmol

    U    = 75              ;    % BTU/hr-ft^2-oF
    rhocp = 53.25          ;    % BTU/ft^3
    R    = 1.987           ;    % BTU/lbmol-oF
    V    = 750             ;    % ft^3
    F    = 3000            ;    % ft^3/hr
    Caf  = 0.132           ;    % lbmol/ft^3
    Tf   = 60              ;    % oF

    A = 1221               ;    % ft^2

    ra   = k0*exp(-Ea/(R*(T+460)))*Ca;
    dCa  = (F/V)*(Caf-Ca)-ra;
    dT   = (F/V)*(Tf-T)-(dH)/(rhocp)*ra...
            -(U*A)/(rhocp*V)*(T-Tj);

    dx =[dCa;dT];
```

Figure 1. File saved as **reactor.m**

Remarks:
1. We treat T_j as an argument/parameter. This is in anticipation that we will be varying T_j later as an input/manipulated variable.
2. The arguments **x** and **dx** are column vectors for state and derivative, respectively.
3. Writing a model first for direct ODE45 implementation is advisable, specially for complex processes. This way, one can check the validity of the model, prior to its incorporation to a Simulink model.

IV. Write an S-function file.

This file will also be saved as an m-file. It contains the protocol in which Simulink can access information from Matlab.

For our example, we show one such S-function file in Figure 2. We will save this file as **reactor_sfcn.m**.

```
function  [sys,x0,str,ts]=...
          reactor_sfcn(t,x,u,flag,Cinit,Tinit)
```

```
switch flag

    case 0  % initialize

        str=[]                      ;
        ts = [0 0]                  ;

        s = simsizes                ;

            s.NumContStates = 2     ;
            s.NumDiscStates = 0     ;
            s.NumOutputs = 2        ;
            s.NumInputs = 1         ;
            s.DirFeedthrough = 0    ;
            s.NumSampleTimes = 1    ;

        sys = simsizes(s)           ;

        x0 = [Cinit, Tinit]         ;

    case 1                          % derivatives

        Tj  = u                     ;
        sys = reactor(t,x,Tj)       ;

    case 3  % output

        sys = x;

    case {2 4 9}                    % 2:discrete
                                    % 4:calcTimeHit
                                    % 9:termination
        sys =[];

    otherwise

        error(['unhandled flag =',num2str(flag)])   ;

end
```

Figure 2. File saved as **reactor_sfcn.m**.

Let us deconstruct the S-function file given in Figure 2 to understand what the file needs to contain.

1. <u>The first line specifies the input and output arguments</u>.

```
function  [sys,x0,str,ts]=...
          reactor_sfcn(t,x,u,flag,Cinit,Tinit)
```

As it is with any Matlab functions, the variable names themselves are not as crucial as the positions of the variables in the list.

a) input arguments

    (1) `t` - the time variable

    (2) `x` - the column-vector of state variables

    (3) `u` - the column-vector of input variables (whose value will come from other Simulink blocks)

    (4) `flag` - indicator of which group of information and/or calculations is being requested by Simulink.

    There are six types of request that Simulink performs, each of which is designated by an integer number:

`flag` value	Job/Data Request
0	**_Initialization:_** a) Setup of input/output vector sizes and other setup modes b) Specification/calculation of initial conditions for the state variables.
1	**_Derivative Equation Updating:_** a) Calculations involving input vectors b) Calculation of the derivatives
2	**_Discrete Equation Updating_** (will not be used for our example)
3	**_Output Calculations:_** Evaluating output variables as a function of the elements of the state vector (and in some case, also the elements of the input vector)
4	**_Get Time of Next Variable Hit_** (will not be used for our example)
9	**_Termination:_** Additional routines/calculations at the end of the simulation run. (will not be used for our example)

    (5) `Cinit,Tinit` - additional supplied parameters.

    In our case, these are the initial conditions for concentration and temperature.

Note: We do not specify what the values of the input arguments are. Their values will be specified by Simulink during a simulation run.

b) output arguments

(1) `sys` - the main vector of results requested by Simulink. Depending on the `flag` sent by Simulink, this vector will hold different information.

If **flag** $= 0$	**sys = [a,b,c,d,e,f,g]**
	where,
	  a = number of continuous time states
	  b = number of discrete time states
	  c = number of outputs (*Note: this is not necessarily the number of states*)
	  d = number of inputs
	  e = 0 (*required to be* 0*, not currently used*)
	  f = 0(no) or 1(yes) for direct algebraic feed through of input to output. (*this is relevant only if during flag=3, the output variables depend algebraically on the input variables.*)
	  g = number of sample times. (*for continuous process, we set this equal to* 1)

If **flag** $= 1$	**sys =** a column vector of the derivatives of the state variables
If **flag** $= 3$	**sys =** a column vector of the output variables
If **flag** $=$ 2,4,9	since these flags are not used in our example, they can just send out a null vector: **sys=[ ]**

The next set of 3 output arguments are needed by Simulink only when **flag** $= 0$, otherwise they are ignored:

(2) **x0** - column vector of initial conditions.

(3) **str** - need to be set to null. This is reserved for use in future versions of Simulink.

(4) **ts** - an array of two columns to specify sampling time and time offsets. Since our example will deal only with continuous systems, this will be set to **[0 0]** during initiation phase.

2. After the first line, the S-function file is split into the different cases determined by **flag**. As shown in Figure 3, we show the bare structure of the "containers" for the different cases. We have left out the details for case 1, 2 and 3. For case 2, 4, and 9, we simply set **sys=[]**. The last two lines to catch an exceptional case where a bug occurs during the Simulink run.

```
switch flag

    case 0                              % initialize

      %...

    case 1                              % derivatives

      %...

    case 3                              % output

      %...

    case {2 4 9}                        % 2:discrete
                                        % 4:calcTimeHit
                                        % 9:termination
        sys =[];

    otherwise

        error(['unhandled flag =',num2str(flag)])   ;

 end
```

Figure 3.

Now, let us fill the details.

For case 0 (initialization),
a) define **str**, **ts** and **x0**

```
            str=[]                      ;
            ts = [0 0]                  ;
            x0 = [Cinit, Tinit]         ;
```

b) create a row vector which specifies the number of inputs and outputs, etc.
To aid in this, we invoke the **simsizes** command.
Without arguments, **simsizes** will creates a strucure variable which we can then fill with the required values:

```
 s = simsizes                          ;
```

6

```
s.NumContStates   = 2   ;
s.NumDiscStates   = 0   ;
s.NumOutputs      = 2   ;
s.NumInputs       = 1   ;
s.DirFeedthrough  = 0   ;
s.NumSampleTimes  = 1   ;
```

Using the command **simsizes** again with the structure variable as the argument actually translates the values in the structure, **s**, into a row vector which gets sent to Simulink via **sys**:

```
sys = simsizes(s)           ;
```

For case 1 (derivative calculations)

We set the input **u** to **Tj** and then apply it to the m-file we wrote earlier, i.e. **reactor.m**:

```
case 1                          % derivatives

    Tj  = u                     ;
    sys = reactor(t,x,Tj)       ;
```

For case 3 (output calculations)

```
case 3                          % output

    sys = x;
```

V. Insert the S-Function block into the Simulink.

In the Simulink Library browser, go to the [**User-Define Functions**] subdirectory. Then drag-drop the **S-Function** block (see Figure 4).

Double-click on the S-function block and fill in the parameters. Change the S-function name to **reactor_sfcn**. Also, fill in the parameters. In our case, we input **0.1,40** (which is the value for **Cinit** and **Tinit**) as shown in Figure 5.
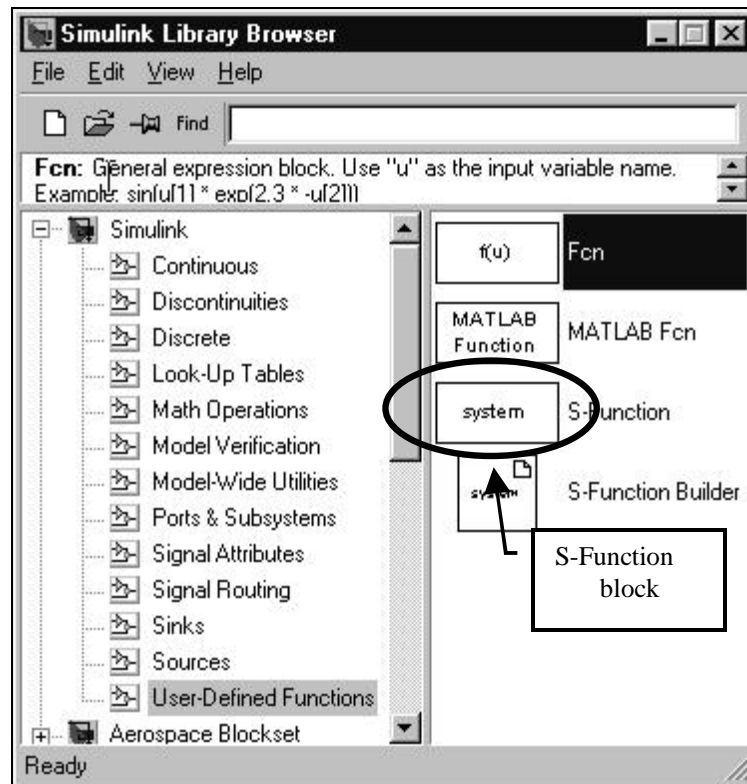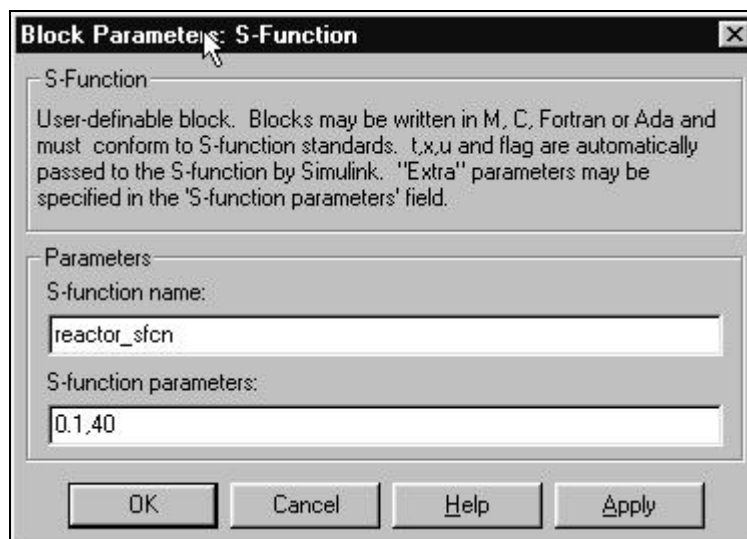
Figure 4.

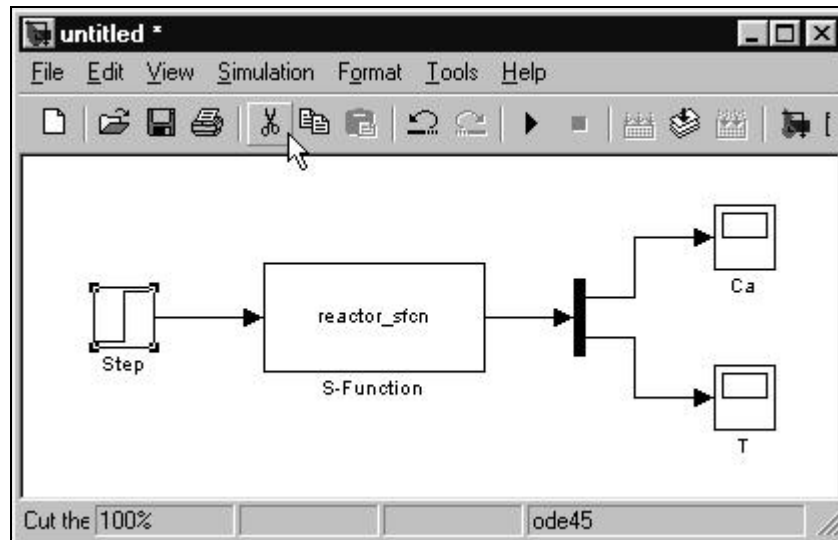Figure 5.

VI. Add other Simulink blocks and simulate.

Figure 6.

Remark: In figure 6, we include a **demux** block (which stands for demultiplexer) to split the output vector to the 2 elements. In other applications where the input vectors has more than one element, we need a **mux** block (which stands for multiplexer). Both **mux** and **demux** blocks reside in the **Signal Routing** subdirectory of the Simulink Library browser.

<div align="center">

Short Tutorial on Matlab

(©2004 by Tomas Co)

</div>

Part 6. Finding Steady States and Linearization via Simulink®

1. **Consider the biochemical system,**

   (based on process developed in B. Wayne Bequette, "*Process Control: Modeling, Design and Simulation*", Prentice Hall, 2003, pp. 631-634.)

$$\frac{dx_1}{dt} = (\mu - D)x_1$$

$$\frac{dx_2}{dt} = D(x_{2f} - x_2) - \frac{\mu x_1}{Y}$$

$$\mu = \frac{\mu_{\max} x_2}{k_m + x_2 + k_1 x_2^2}$$

2. **Build a Simulink model**

```
function    dx = bioreactor(t,x,D,x2f)
%
%    model for bioreactor process
%    where,   x1 = biomass concentration
%             x2 = substrate concentration
%             D  = dilution rate
%             x2f= substrate feed

    x1 = x(1)                                ;
    x2 = x(2)                                ;

    mumax    = 0.53            ;    % hr^(-1)
    km       = 0.12            ;    % g/liter
    k1       = 0.454           ;    % liter/g
    Y        = 0.4             ;    %

    mu  = mumax*x2/(km+x2+k1*x2^2)       ;

    dx1 = (mu - D)*x1                    ;
    dx2 = D*(x2f-x2)-mu*x1/Y             ;

    dx = [dx1;dx2]                       ;
```

<div align="center">

Figure 1. m-File for Bioprocess System

</div>

```
function  [sys,x0,str,ts]=         ...
     bioreactor_sfcn(t,x,u,flag, ...
     x1_init,x2_init)

switch flag

    case 0  % initialize

        str=[]                      ;
        ts = [0 0]                  ;

        s = simsizes                ;

            s.NumContStates  = 2   ;
            s.NumDiscStates  = 0   ;
            s.NumOutputs     = 2   ;
            s.NumInputs      = 2   ;
            s.DirFeedthrough = 0   ;
            s.NumSampleTimes = 1   ;

        sys = simsizes(s)           ;

        x0 = [x1_init, x2_init]     ;

    case 1  % derivatives

        D   = u(1)                  ;
        x2f = u(2)                  ;
        sys = bioreactor(t,x,D,x2f);

    case 3  % output

        sys = x                     ;

    case {2 4 9}    % 2:discrete,
                    % 4:calcTimeHit,
                    % 9:termination

        sys =[]                     ;

    otherwise
        error(...
           ['unhandled flag =',...
            num2str(flag)])         ;

end
```
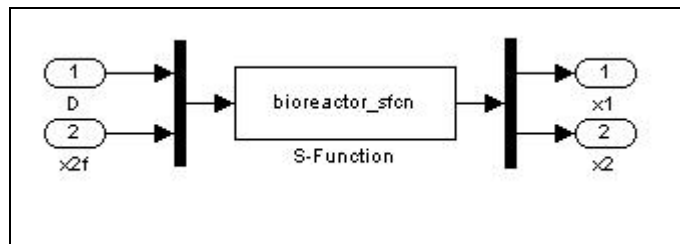
Figure 2. Code for S-function

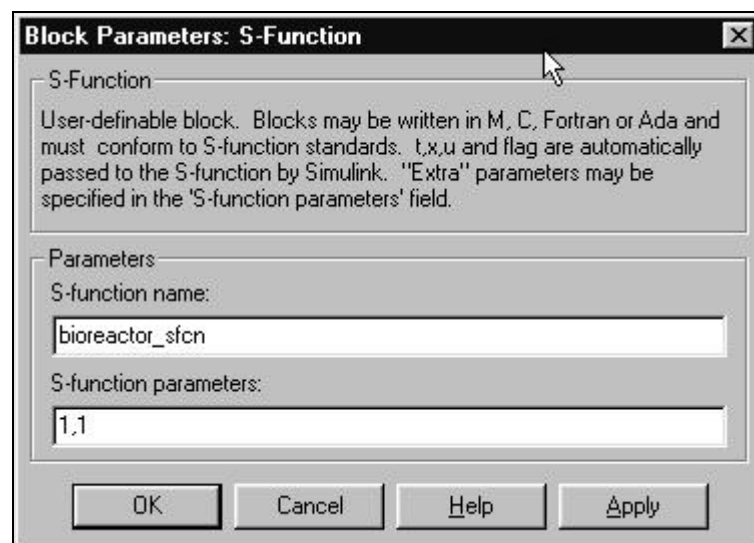Figure 3. Simulink model: bioreactor_sys.mdl

Figure 4. Set Parameters (in our case, initial conditions)

3. Use the **trim** function to get steady state.

a) set some more parameters: i.e. we want to fix the input values of D=0.3 and x2f=4.0

```
>> X0=[];
>> U0=[0.3;4];
>> Y0=[];
>> IX=[];
>> IU=[1;2];
>> IY=[];
```

Remarks:

i) **X0**, **U0** and **Y0** are the state vector, input vector and output vector that will be fixed while the function attempts to find the steady state. Note that since we will not constrain the states and outputs, we can set these to null.

ii) **IX, IU** and **IY** indicates which values of **X0, U0** and **Y0** will be held fixed. In our case, we want both input vector to be fixed, so we set **IU = [1;2]**.

b) run the trim function:

```
>> [X,U,Y,DX]=TRIM('bioreactor_sys',X0,U0,Y0,IX,IU,IY);
>> X

X =

    0.9943
    1.5141
```

Thus, the function found X=(0.9943,1.5141) as the steady state.

4. Linearization via the **linmod** function.

```
>> [A,B,C,D]=linmod('bioreactor_sys',X,U0);
```

which results in the following:

```
A =
    0.0000   -0.0678
   -0.7500   -0.1304

B =
   -0.9943        0
    2.4859   0.3000

C =
    1.0000        0
         0   1.0000

D =
    0    0
    0    0
```